Driver state estimation by using graphical-based model toward advanced driver assistance systems

Dissertation by

NGUYEN THANH TUNG

Submitted in Partial Fulfilment of the Requirements

for the Degree of Doctor of Philosophy

in Mechanical Systems Engineering

名古屋大学

NAGOYA UNIVERSITY

Graduate School of Engineering

Nagoya University

JAPAN

December 2020

Dissertation Committee

Tatsuya SUZUKI

Professor

Koji MIZUNO

Professor

Koji OGURI

Professor

Hirofumi AOKI

Professor

Contents

Acknowledgements

First and foremost, I would like to express my sincerest appreciation to my supervisors, Professor Hirofumi Aoki and Professor Tatsuya Suzuki. This work would not be completed without their professional guidance and patience in supervision. They have instructed me how to broaden my scope of interest and to complete the present study. Furthermore, their understanding and value supports not only in research but also in daily life helped me have great years in Japan.

I would like to express my appreciation to Dr. Issey Takahashi and Mrs. Izumi Araki. They are the best Japanese friends I have during my time in Japan. Dr. Takahashi has helped me a lot not only in the research but also in my early life of Ph.D student. Mrs. Araki and I have worked together in almost all of the experiments. She also helped me to expand my knowledge in the medical field which is extremely useful for my research. I would also like to express my gratefulness to other professors in the Suzuki Laboratory, my knowledge has been expanded significantly through their lectures and insightful comments.

In addition, I greatly thank all members of Human Factors and Aging Laboratory for general laboratory assistance. In particular, I would like to thank the members who have cooperate with me in various experiments: Dr. Makoto Inagami, Mr. Kunimoto Aoki, Mr. Hirano Akio, Mr. Masayuki Shimizu for their assistance and advices during experiment.

I appreciate Ministry of Education and Training (Vietnam) for providing me with a scholarship for the Ph.D course. With this financial support, I would focus on the research and completed this thesis. I would like to express my appreciation to my colleagues in the Department of Automotive Engineering (Hanoi University of Science and Technology, Vietnam) who have given a lot of advice to live and study before going to Japan.

I wish to express thanks to my Vietnamese friends in Japan, Dr. Le Anh Son, Prof. Ngo Van Nong, Mr. Nguyen Truong who helped me so much and encouraged me to complete this study.

Finally, I would like to thank all members of my family, they are the most important people in my life. They are always there for me, whose love, care and sympathy helped me go over the hardest time in Japan.

Nagoya University, December 2020

NGUYEN THANH TUNG

List of Published Papers

Chapter 7

T. T. NGUYEN et al. (2017). "Development of an automated vehicle stop system for cardiac emergencies". In *ASTESJ* Volume 2, Number 3, page 669-673.

Chapter 5

T. T. NGUYEN et al. (2021). "Driver state detection based on cardiovascular system and driver reaction information using a graphical model". In *Journal of Transportation Technologies* (16 pages, accepted).

List of Figures

List of Tables

Chapter 1

Introduction

1.1 Background

The invention of the motor vehicle in the late 1800s has significantly changed how the world operates. With the widespread use of automobiles from the 1900s, many other technologies started to evolve to catch with the new demands: mechanical engineering, road infrastructure, in-vehicle equipment and driver education. The advanced systems embedded inside the vehicle have freed humans from most of the hard work of driving and allow them to attend more on the other things such as: conversation, enjoy music, etc. It is not uncommon to see a driver surfing the web or texting while driving these days. According to common law, such actions are considered inappropriate to driving since they can distract the driver from their primary task and expose to a higher risk of accidents. In a recently published report, the World Health Organization (W.H.O , 2020) showed that there are around 1.35 million fatalities every year because of road traffic accidents.

1.1.1 Traffic accidents

According to W.H.O, the factor that contributes most to a large number of accidents is human error: speeding, driving under the influence of psychoactive substances, distracted driving. Other factors are nouse of safety equipment (helmets, seatbelt,

and child restrains), unsafe road infrastructure, inadequate post-crash care, and inadequate law enforcement of traffic laws.

The combined efforts of government, scientists, automotive makers, and society have made big progress in reducing the number of road traffic deaths in high- and middle-income countries. But the progress has been little in low-income countries.

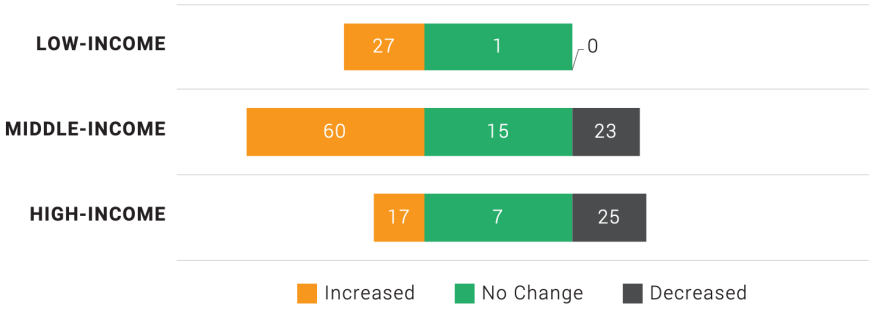

Figure 1.1: Change in the number of road traffic deaths (2013-2016) (source: W.H.O , 2018)

In Japan, the number of traffic accident fatalities fell in 2019 to 3215, a three-year consecutive decrease and the lowest figure since data were recorded in 1948 (data taken from Nippon.com). Even though the number of fatalities fell in total, the proportion of senior citizens (aged 65 and over) remained high (over 50%). The common causes of accidents are checking the surroundings, using the phone, checking the pedestrians, and drinking driving.

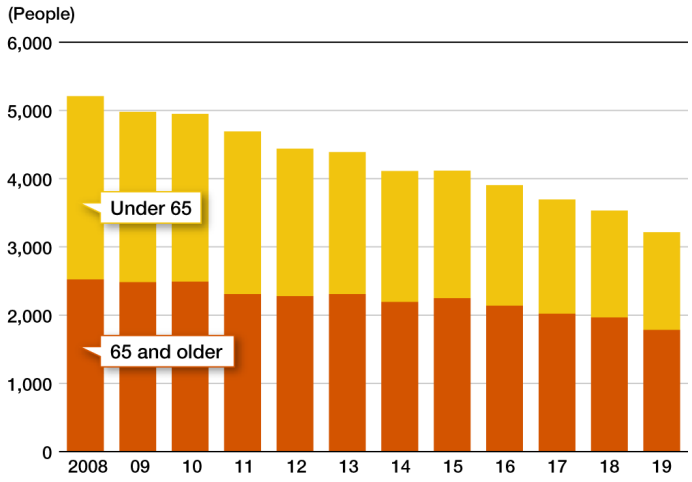

Figure 1.2: Traffic fatalities among Japanese citizens (source: Nippon.com)

The leading factors also vary depending on the countries. In Vietnam, majority of the traffic accidents related to violating the laws (on the wrong lane) (accounted for more than 20%). The total of road crashes still increases along with the increase of the demand for transportation.

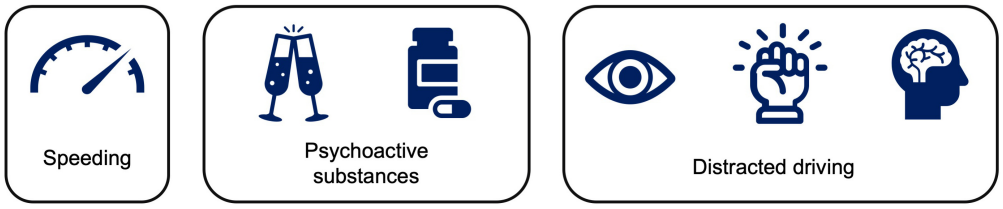

Figure 1.3: The most contributing factors to road accidents

Effects of speeding

Speeding violation is related to law enforcement on the road to keep the driving safety. The reasons for speeding come from various aspects: ages, gender, types of jobs, driving culture, etc. Recent studies also found a correlation between strong emotions (anger, anxiety, and contempt) and maladjusted behaviors (aggressive and road rage) (Roidl et al. , 2014).

Effects of psychoactive substances

In many countries, the number of fatalities due to the influence of alcohol and drugs is always among the highest. Alcohol decreases the reflexes and thus decreases the reaction response of the driver. It can also reduce hand and foot coordination and lead to driving errors. Furthermore, alcohol has effects on the brain and cognitive functions which lead to reduce driver vision, concentration and comprehension (the ability to make decisions). Drug abuse (narcotics, marijuana, methamphetamine, etc) often find in young drivers but also find on other age groups. Another emerging topic which is received public debation is the treatment drug (Hours et al. , 2008).

Effects of distracted driving

Distracted driving is any activity that diverts attention from driving, including texting, conversation, drinking, using mobile, etc. According to the National Highway Traffic Safety Administration (NHTSA—United States), there are three types of driver distraction:

- **Vision**: taking your eye off the road;
- **Manual**: taking your hand off the driving wheel;
- **Cognitive**: taking your mind off the driving.

Various studies have attempted to resolve/detect the distraction or inattention (D'Orazio et al. , 2007; Fletcher and Zelinsky , 2009; Liao et al. , 2016).

1.1.2 Driver assistance system

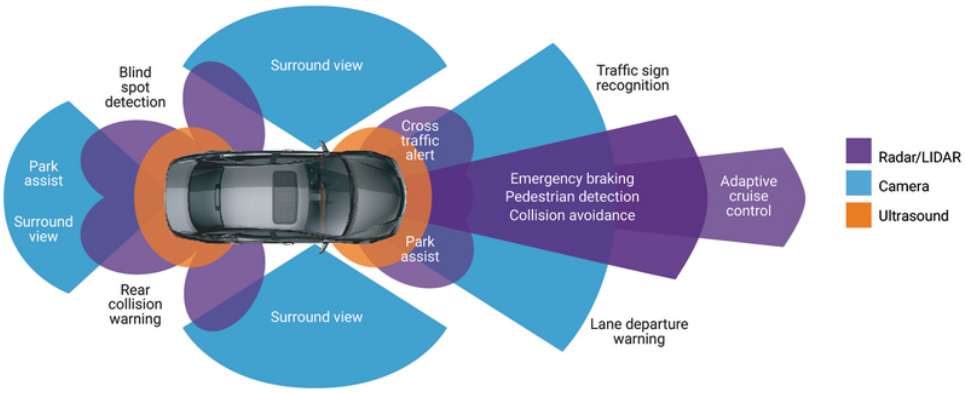

Figure 1.4: Example of Advanced Driver Assistance Systems

(source: Synopsys, Inc.)

Besides road infrastructure improvement and traffic law enforcement by the government, automaker companies also equip vehicles with anti-crash protection options, such as collision avoidance systems, emergency brake assistance, lane-keeping system, etc. The NHTSA (Forkenbrock and Snyder , 2015) released a protocol to test emergency braking at a speed of 25 mph ($\tilde{4}$0 kph) with a stopped lead object and 35-45 mph ($\tilde{5}$6-72 kph) with a slower/decelerating lead object, which is suitable for most traffic cases. Still, those systems have their limitations, including upper-speed thresholds, swaying vehicles, when driving uphill, etc. The best performance must be achieved by keeping drivers' attention on the driving task.

1.2 Objective and Construction

1.2.1 Objvetive

It can be seen that of all the mentioned factors, driver's state keeps an major role in safety driving. The main objective of this study is to implement a proper method to estimate driver states by using non-invasive sensors and in-vehicle data. The proposed method can be used for risk estimation related to the driver health condition. Based on that, hopefully, the method can provide a tool in the development and improvement of future driver assistance system.

1.2.2 Dissertation construction

This dissertation is organized as the following eight chapters. Chapter 1 introduces the background of traffic accidents. In Chapter 2, various of driver assessment methods are presented and discussed. Then the effects of driving tasks and driver states on the physiological indices were investigated on real-world driving in Chapter 3. Chapter 4 provides the background and the advantages of the graphical models in exploring complex systems. In Chapter 5, a graphical-based model is developed to detect the surprise state of the driver in case of pedal misapplications. Chapter 6 will discuss about another possible application of the graphical-based method on detecting drowsiness and the preliminary result. In Chapter 7, a concept of the driver assistance system was demonstrated and the possibility of using the proposed method in improving the system. Conclusion and remarks of future work are given in Chapter 8. The relationship between chapters is showed in Figure 1.5 as follows.

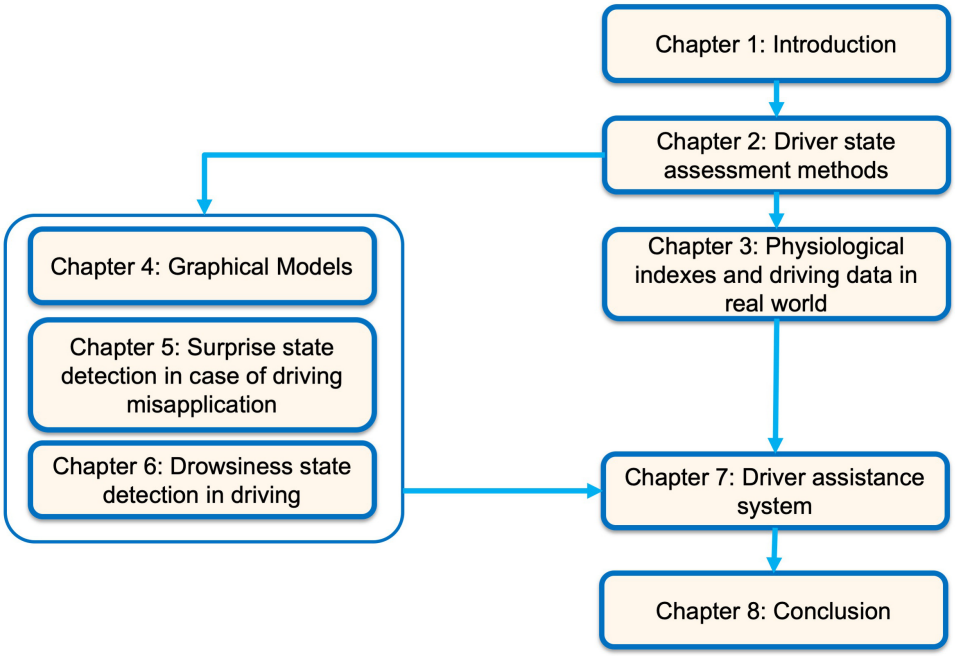

Figure 1.5: Dissertation outline

Chapter 2

Driver state assessment methods

The purpose of this chapter is to provide the background of all possible metrics to assess the driver states. Driver states are considered as one of the main contributing factors to driving safety. All over the world, researchers have extensively conducted studies related to driver assessment. Existing and cutting-edge methods and technologies will be mentioned. Figure 2.1 shows an example of equipment which are attached to the driver and installed inside the vehicle to collect driver's bio-metrics and driving operation data: EEG headset, ECG electrodes attached to the chest, driver recorder camera, and driving operation data.

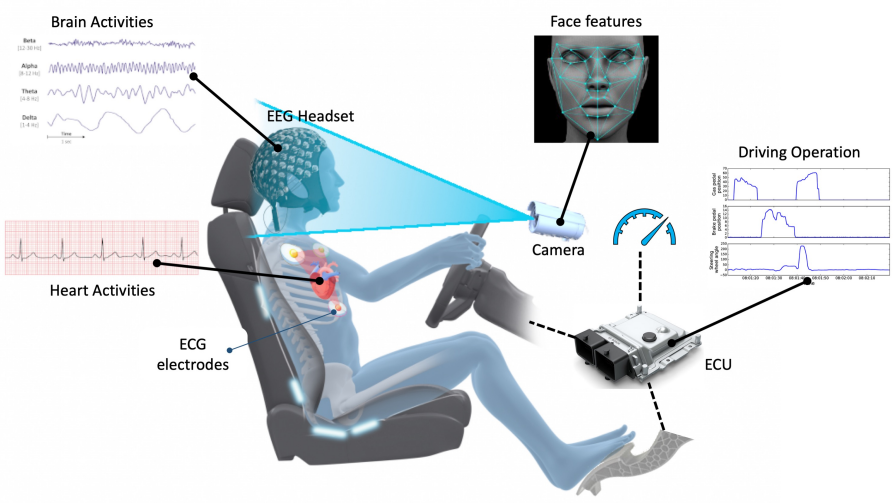

Figure 2.1: Driver's features and Driving features collected inside the vehicle

2.1 Physiological indices

Physiology is a sub-discipline of biology which studies the functions and mechanisms of a living system. When using biosignal measurement in evaluating the driving comfort, driving workload, and the usability of in-vehicle systems, changes in the physiological state of the driver are measured. The knowledge in driver physiological measures often come from the medical field which includes Central nervous system activity (or Brain activity), Autonomic nervous system activity (or Cardiac/Heart system), Visual system, and other physiological indices.

2.1.1 Brain activites

Electroencephalogram - EEG

Electroencephalogram (EEG) is one of the oldest methods for non-invasive observation of human brain-activity patterns. The EEG amplifies the electrical potential difference that occur between two electrodes attached on the scalp. The cerebral cortex contains billions neurons and they are connected by synapses to form a network. The human brain is always active electrically, so potential changes that are measured by EEG are also occurring constantly.
Frequency bands of EEG which interest many studies are:

- The delta band (0.5-4 Hz)
- The theta band (4-8 Hz)
- The alpha band (8-13 Hz)
- The beta band (13-30 Hz)
- The gamma band (>30 Hz)

Figure 2.2 shows an example of EEG headset setup and some frequency bands of EEG signals.

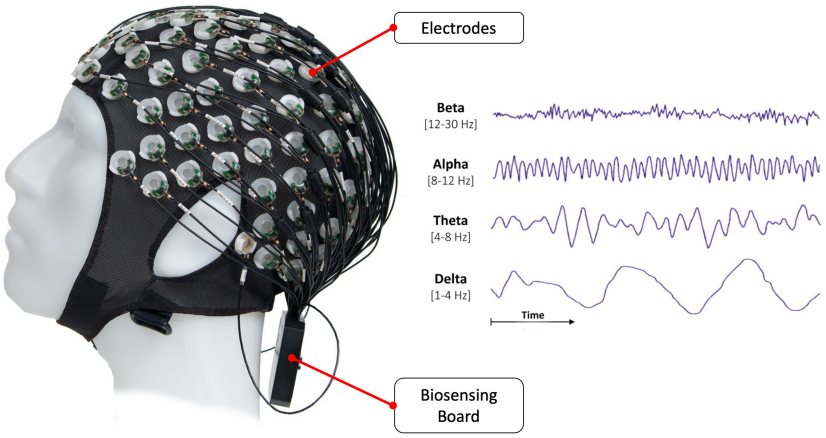

Figure 2.2: EEG Headset and EEG signal

Depend on the arousal state, the beta band and gamma band can be dominant. On the other state, the alpha band can be observed. In car driving, the amplitude in the alpha, theta, and delta bands changes significantly due to different states such as fatigue or sleepiness. Many studies have used EEG as an indicator to detect driver mental states, fatigue, drowsiness, etc (Lal et al. , 2003; Min et al. , 2017; Nguyen et al. , 2017; Zeng et al. , 2018). Therefore, sometimes EEG is considered as the standard reference for the other methods when estimating the driver state. The disadvantage of EEG are the sensitivity of the electrodes to the head movement and to receive better understanding of the brain activities, more electrodes are needed. So that most of the studies using EEG are conducted in the development phase, it is difficult to apply in commercial/practical use.

Functional Near-infrared spectroscopy - fNIRS

Functional Near-infrared spectroscopy (fNIRS) is a method that evaluates the blood flow changes in the brain. In the fNIRS, the near-infrared light is emitted from

the scalp and measure the reflected light on the scalp. It estimates the changes in the concentration of oxygenated and deoxygenated hemoglobin in the cerebral cortex. These changes in the hemoglobin concentration in blood are associated with the brain activities. Compare to the other techniques on research brain, fNIRS resolution is lower but the equipment is more compact and allows head movement more freely. There have been many reports of using fNIRS to evaluate driver state (Fakhrhosseini et al. , 2015; Xu et al. , 2017; Tanveer et al. , 2019). However, the measurement is affected by many factors such as the probe stability, hair, and the scalp blood flow, calibration and attention are required when interpreting the results.

2.1.2 Cardiac system

Electrocardiogram - ECG

Electrocardiogram (ECG) is a graph of voltage versus time of the electrical activity of the heart using electrodes placed on the skin of the subject. There are three main components of the ECG signal:

- The P wave represents the depolarization of the atria;
- The QRS complex represents the depolarization of the ventricles;
- The T wave represents the repolarization of the ventricles.

The interval of the R peak of the QRS complex is called the RR interval (RRi). Figure 2.3 shows the heart structure and a single normal ECG pattern. Based on the RRi value, the heart rate (HR) per minute is calculated. In clinical, a complex 12-lead ECG is used to record the heart's electrical potential from 12 different angles. The results will be used to monitor and give diagnose by the physicist and doctor. In other fields such as human factors, lead-II configuration is often used due to its simple requirement: 2 electrodes on both sides of the heart and an area for

grounding.

The HR is regulated by the 2 branches of the autonomic nervous system (ANS). The HR increases upon the activation of the cardiac sympathetic nervous system (SNS) which stimulates the body's fight-to-flight response. On the other hand, The parasympathetic system (PSNS) is responsible for stimulation of "rest-and-digest" or "feed and breed" activities that occur when the body is at rest and decrease the HR. In general, HR is used as an index for physical and mental strain. HR and temporal HR changes have been reported in mental effort, tension, fatigue, arousal studies.

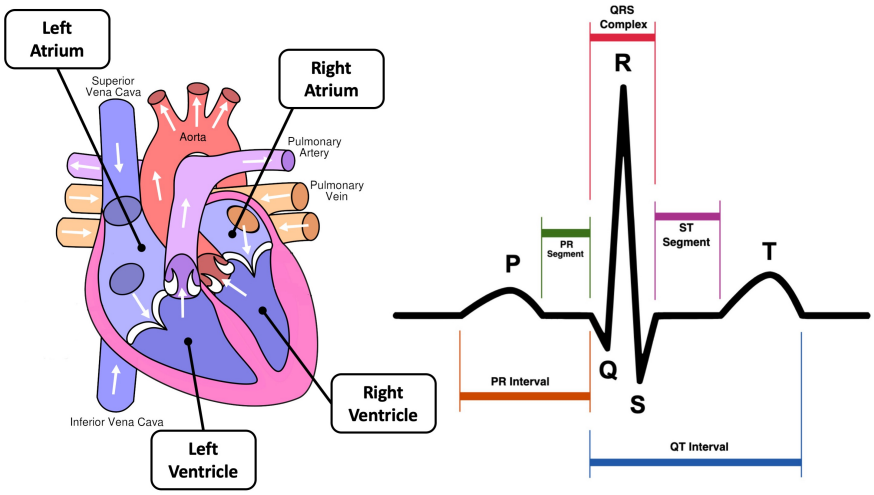

Figure 2.3: Heart structure (left) and ECG waveform (right)

(source of ECG waveform: https://en.wikipedia.org/wiki/Electrocardiography)

Heart-rate Variability - HRV

Heart-rate Variability (HRV) is the variation of the instantaneous HR. The HRV indices can be calculated in time-series domain, frequency domain, and non-linear domain. In medical fields, the standard period to compute HRV is often 5 minutes. But recent studies also discussed about shorter period can be used in some specific cases (Esco and Flatt , 2014; Pecchia et al. , 2018). The definitions and quantifying methods of HRV indices vary among researchers and make comparison of the results

difficult. But the using HRV indices is still one of the strong techniques in assessing human states. Table 2.1 shows some of the popular HRV indices.

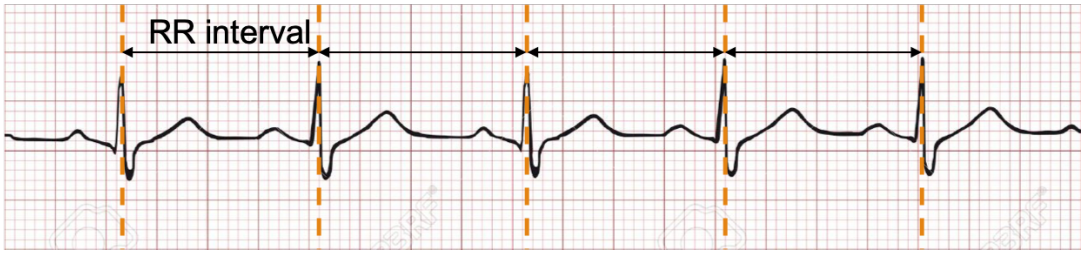

Figure 2.4: RR interval extracted from ECG waveform

Table 2.1: Summary of some popular HRV parameters

Parameter	**Unit**	**Description**
Time Domains		
meanRR	ms	Mean of RR intervals
SDNN	ms	Standard deviation of RR intervals
meanHR	1/m	Mean of Heart rate
STD HR	1/m	Standard deviation of instantaneous Heart rate values
RMSSD	ms	Square root of the mean squared differences between successive RR intervals
Frequency Domains		
VLF, LF & HF peaks	Hz	Peak frequencies for VLF, LF and HF bands
VLF, LF & HF powers	ms^2	Absolute powers of VLF, LF and HF bands
LF/HF	-	Ratio between LF and HF band powers
Total power	ms^2	Total spectral power
Non-linear Domains		
SD1, SD2	ms	Standard deviations of the Poincaré plot
ApEn	-	Aproximate Entropy
SampEn	-	Sample Entropy

Photoplethysmogram - PPG

A photoplethysmogram (PPG) is an optically method that can be used to detect blood volume changes in the microvascular bed of tissue. A PPG is often obtained by using a pulse oximeter which illuminates the skin and measures changes in light absorption. The same technique is used in fNIRS. Unlike the fNIRS retrieve activities from blood veins near the brain, PPG is often referred to the blood veins of the body and thus getting the pulse rate or heart rate. By using PPG, instantaneous HR and SpO_2 can be retrieved and used for further analysis. Due to the compactness of the setup, PPG sensors are widely used in both academic studies (Yoshino et al. , 2007; Tamura , 2019) and commercial products (sport watch, health monitoring devices). The sensor positions are not only on the thump but also on the other body positions such as nose, temple, earlobe, and wrist.

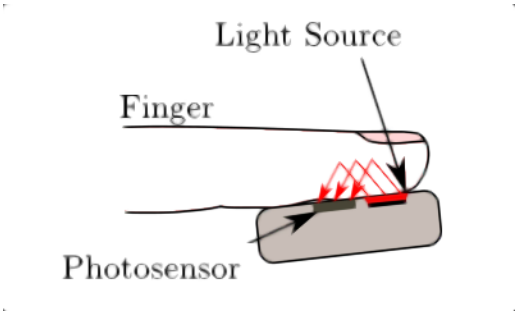

Figure 2.5: PPG sensor in finger

2.1.3 Visual system

Eye movement

Eye movement is measured by the optical method and the electrooculography (EOG) method. The optical method adopts the image measurement such as camera, video image processing. In this method, the pupil diameter can also be measured. The EOG method detects a bioelectric phenomenon and measuring the eye movement

by detecting the difference in the electrostatic capacitance of the cornea and the retina by sensors attached around the eyes.

The optical methods are widely used due to its simple setup. Studies about eye movement can be focused on either voluntary movement or involuntary movement. Voluntary movement can be seen as gaze direction, saccade, and eye rotation. Involuntary movement involves with the unintentionally movement of the eyes. There have been many studies using those characteristics to detect drive states (Obinata et al. , 2008; Le et al. , 2019). Eye movement also can be used at the same time with the facial expression method to detect driver emotions, fatigue, and drowsiness. The disadvantage of this method is the sensitivity of the camera to the surrounding environment (light) and the need of calibration for different positions.

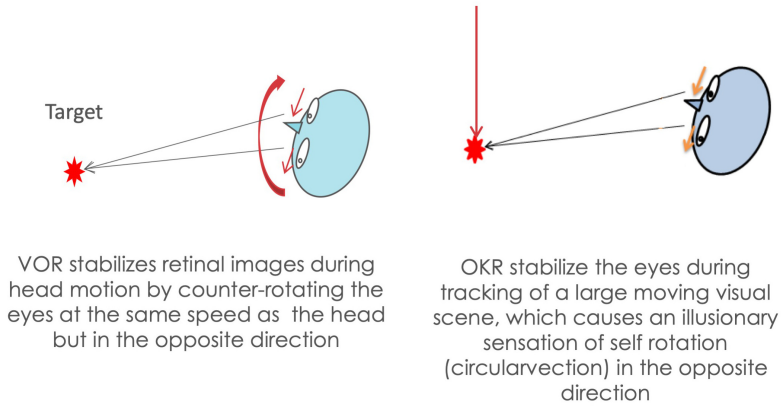

Figure 2.6: Involuntary eye movement

Eye blink

Eye blink can be measured by using electrical potential changes using EOG method or by using the image processing. In studies on automobile, the arousal state is evaluated by indices such as eye-closing time, blink rate, and blink waveform. Eye blink is also a useful index for evaluating other driver states such as cognitive state, attention state, and workload (Danisman et al. , 2010; Benedetto et al. , 2011).

Pupil

The pupil is a hole located in the center of the iris of the eye that allows light to go through the retina. The pupil reaction (constriction or dilation) is the response to the surrounding light (bright or dark). There is also a near reaction where the pupil becomes smaller when looking object at a near distance. Moreover, the pupillary dilator is also controlled by the sympathetic nerves, so that the pupil is constricted when the subject feels strong sleepiness or fatigue, and is dilated when the subject becomes excited.

2.1.4 Other physiological indices

Other physiological indices can be used in driver state assessment are blood pressure (BP), respiration rate, galvanic skin response (GSR), etc. These indices are often measured incorporate with other physiological indices to evaluate and detect driver states.

2.2 Driving-based indices

Beside biometrics, driving-based indices are also widely used in driver state detection. In-vehicle sensors provide not only the vehicle dynamic data but also the driver operation data.

2.2.1 Longitudinal indices

Velocity metrics

Speed metrics are the most commonly used metrics in driving behavior studies. The vehicle velocity is often inferred from the wheel sensors but sometimes GPS data is also used. Typical metrics are mean velocity, velocity variation and maximum velocity.

Acceleration is computed by differentiating the vehicle velocity. When the velocity data is discrete, a difference calculation is applied. The other method to obtain the acceleration of the vehicle is using an accelerometer. In such case, the axis of the sensor must be aligned with the longitudinal axis of the vehicle.

Another factor needs to be considered is the differentiated value of the acceleration: Jerk. The vehicle occupants are sensitive to the jerk of the vehicle in motion. The jerk can be used to detect the onset of the change in acceleration.

Reaction time

The acceleration or deceleration of the vehicle depends on the pedal operation of the driver: move his/her leg from the brake pedal to the gas pedal and step on it; or vise versa, release the gas pedal, move the leg to the brake pedal to slow down or stop.

There are many definitions of the onset and the end of the response time. It can begin with the event trigger or when the driver release his/her gas/brake pedal.

It depends on what kind of the signal is available in the study. Reaction time is still one of the interesting measures when it comes to traffic safety (Taoka , 1989; Mohebbi and Gray , 2009).

Headway metrics

Distance to the front obstacle is often collected from the sensor put in the front of the vehicle. But distance is not used directly but through its derivation: the headway metrics. Variation of the headway metrics are Time Headway (THW) (Schleuning and Douglas , 2001; Siebert et al. , 2014), Time To Collision (TTC) (Kiefer et al. , 2006), Performance measure for approach and alienation (KdB), and Perceptual Risk Estimation (PRE) (Aoki and Hung , 2011).

The definitions of the headway metrics are different, it is important to use the accurate metric in the specific case. Another considering factor when using headway metrics is the instrumental sensor equipped in the vehicle, the sensor is attached in front of the ego vehicle and detect the rear end of the front vehicle. So that the actual distance value is smaller than the engineering definition of the distance. Also the sensor range and angle detection are limited. It is sometimes difficult to get the data in the real-world experiment. Figure 2.7 shows how to get the longitudinal information from following situation. Tabel 2.2 shows the formulations of some headway metrics with the longitudinal information and driving response.

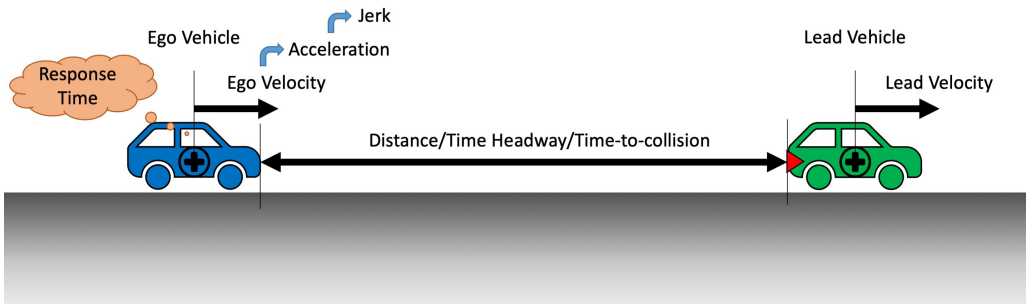

Figure 2.7: Longitudinal indices for driving performance

Table 2.2: Formulas of some Headway metrics

Parameter	**Unit**	**Formula**
Time Headway	sec	$THW = \frac{D}{V_{ego}}$
Time-to-Collision	sec	$TTC = \frac{D}{\lvert V_{ego} - V_{lead} \rvert}$
Perceptual Risk Estimation	$\frac{1}{sec}$	$PRE = \frac{V_r + \alpha V_s + RT(Ap + Af)}{D^n}$

D	-	Distance between ego vehicle and lead vehicle [m]
V_{ego} and V_s	-	Velocity of the ego vehicle [m/s]
V_{lead}	-	Velocity of the lead vehicle [m/s]
$V_r = \lvert V_{ego} - V_{lead} \rvert$	-	Relative velocity between ego vehicle and lead vehicle [m/s]
α	-	constant depend on kinematic perception
RT	-	Reaction time [s]
A_p	-	Deceleration of the lead vehicle [m/s^2]
A_f	-	Foreseen deceleration of the lead vehicle [m/s^2]
n	-	exponent constant depend on the distance perception

2.2.2 Lateral indices

Steering operation

Drivers steer the vehicle appropriately to travel following the curves and change lanes. In other cases to avoid the obstacles, vehicle maneuvering is also needed. Regarding the steering operation, there are steering reaction time and steering movement time. These steering response indices are often used to evaluate the driving performance while activating lane-departure or lane-keeping system. Figure 2.8 shows some of the lateral indices can be acquired during travel.

Steering reversal

Steering reversal is defined as the change of steering direction within a short period. The steering reversal angle must exceed a threshold angle. The threshold values are varying and depend on the studies. If the value is too small, the calculation of steering reversal will be too sensitive to the noise or steering vibration. If the value is too large, the index will not reflect the operation of the driver. Steering reversal can be used as a metric to evaluate task load and distraction (Markkula and Engstrom , 2006; Kountouriotis et al. , 2016)

Steering entropy

Analysis of the time-series of steering angle data can provide some valuable information. Assuming that the drivers peform smooth steering, then the difference between the predicted steering angle and the actual steering angle can be calculated (predicted errors). In case the driver concentrates on the driving, the steering will be smooth and the distribution of predicted errors will be narrow and close to zero. In case the driver is distracted by other non-driving tasks, the distribution will widen. The extent of frequency distribution can be viewed as the degree of entropy (Nakayama et al. , 1999; Boer , 2001).

Lane position and Standard deviation of Lane position

The position of the vehicle on the road is defined as the distance of a certain vehicle feature to a certain road feature. As for the road, the common features are the middle position of the lane, average values of the vehicle trajectory, and the edge of the centerline of the road. As for the vehicle, the features are the middle point of the frontal axle, the edge of tyres, and the central gravity of the vehicle.

The standard deviation of Lane position (SDLP) is the one of the most common feature to evaluate the driving impairment, inattention, driving workload, etc (Peng

et al. , 2013; Verster and Roth , 2014; Liu et al. , 2016). The value indicates the lateral wobbling of vehicles in the selected lane and road section. SDLP can be calculated following way:

- Calculate the mean lateral position (MLP) for the entire drive

$$MLP[X] = \mu = \frac{\sum_i^N X_i}{N}$$

- The standard deviation of Lane position is defined as:

$$SDLP = \sqrt{\sum_i^N (X_i - \mu)^2}$$

where: X_i is the lane position at time i, N is the number of samples taken for the entire drive

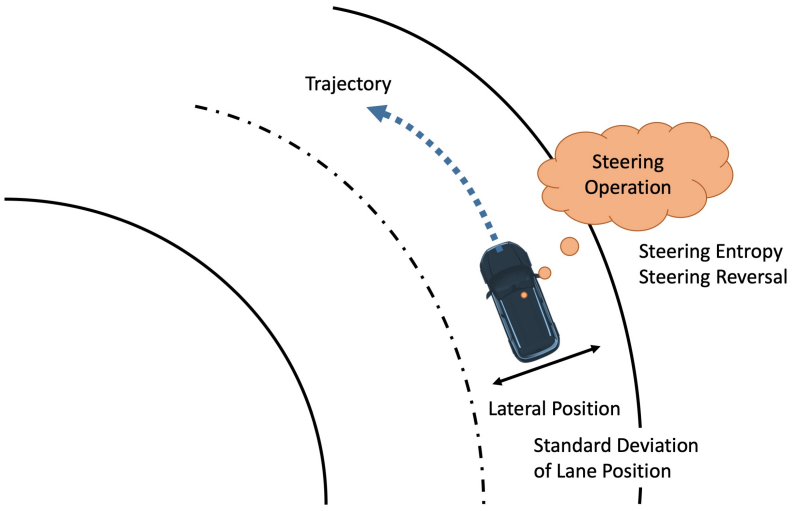

Figure 2.8: Lateral indices for driving performance

2.3 Subjective methods

Besides the physiological measures, the performance-based measures, subjective measures are also widely used to assess the human state in driving. Subjective methods are presented in the form of questionnaires and often given to the subject before and after the experiment to evaluate the change in states. The main advantage of subjective methods is that they are simple and easy to deploy in an experiment. The disadvantage of these methods is that the answers heavily rely on the subject's memory. Furthermore, self-report measures cannot be obtained on a continuous basis like the other mentioned measures.

NASA Task Load Index - NASA-TLX

The NASA Task Load Index (NASA-TLX) was developed by NASA's Ames Research Center as a metric to assess subjective workload (Hart , 2006). The index rates workload based on 6 scales: Mental, Physical, and Temporal Demands, Frustration, Effort, and Performance. This is based on the frame work of task demands, mental resources needed for the performance to meet the demands and the subjective evaluation (effort) of own task performance (the frustration level).

Subjective Workload Assessment Technique - SWAT

The Subjective Workload Assessment Technique (SWAT) was developed by the USAF Armstrong Aerospace Medical Research Laboratory. It evaluates workload based on three dimensions: time load, mental effort load, and psychological stress load. Each of these dimensions has 3 levels: low, medium, and high. The rank order data retrieved from the subjects will be converted to scales [1-100] (Reid and Nygren , 1988). The disadvantages of SWAT are the time required to perform the process and the complexity of the scale calculation (Luximon and Goonetilleke , 2001).

2.4 Conclusion

This chapter has briefly introduced various driver state assessment methods, ranging from the physiological measures, driving-based information to the subjective measures. Each measure has its own advantage and disadvantage. This study will focus on the heart rate and cardiac activities indices because of their wide acceptance in biosignal research and less affected by movement noise while in driving. Driving information is also used because of its importance in safety. The combination of physiological and driving information will lead to a better knowledge driver state in various driving situations.

Chapter 3

Physiological indices and Driving data in real world

3.1 Objectives

Driving is considered as a complex task, demanding both the physical and cognitive resources of the driver. The development of technology has the driver to have a better driving experience. More and more activities beside driving are introduced to the driver and gradually diverse them from the main task and potentially lead to traffic accidents. Human factors focuses on using multiple human aspects and the application of methodologies to solve those problems.

The objective of the study presented in this chapter is to investigate the effect of mental workload and driving difficulty to the response of the cardiovascular system and driving performance of the driver.

Figure 3.1: Preparation for the experiment in Kyosei test track, Okazaki city, Japan

3.2 Methods

3.2.1 Participants

There are 5 participants in this study. All the participants have valid drive licenses. The test drivers are divided into 2 groups: novice drivers and professional drivers. Novice drivers (2 males, 1 female) are young students (aged 20-35) who have little driving experience in Japan (drive less than once a week). The professional drivers (2 males) are middle-age drivers (aged 35-55) who have taken training for vehicle development. The experiment was approved by the Nagoya University's Institute of Innovation for Future Society Ethical Review Board.

3.2.2 Apparatus

Vehicle

All participants drove the same vehicle (Prius) in the test track in turn. The vehicle was equipped with a high-speed CAN computer to record all the operation data of the vehicle.

Driver recorder

Physiological data were recorded by a portable recorder which has the same function with Livo TM4488 (Livo) (Toyota Technical Development Corporation, TTDC, Japan). Livo is a biomedical signal recording system which can record brain activities such as electromyography (EMG) and electrocardiogram (ECG). Instead of sending data to the host computer like Livo, the portable recorder stores ECG data (from electrodes) and PPG data (from sensor in the glasses) directly to the SD card inside which is more compact and easier for in-car driving. Figure 3.2 shows how the ECG is recorded in two systems. The portable recorder ECG recordings used a lead

II configuration at a sample rate of 1000 Hz. Isopropyl alcohol cleaner was used to clean the skin and standard pre-gelled disposable electrodes (Ag/AgCl paste, Vitrode Bs-150) were applied. The start and stop time of the task were recorded by a trigger button.

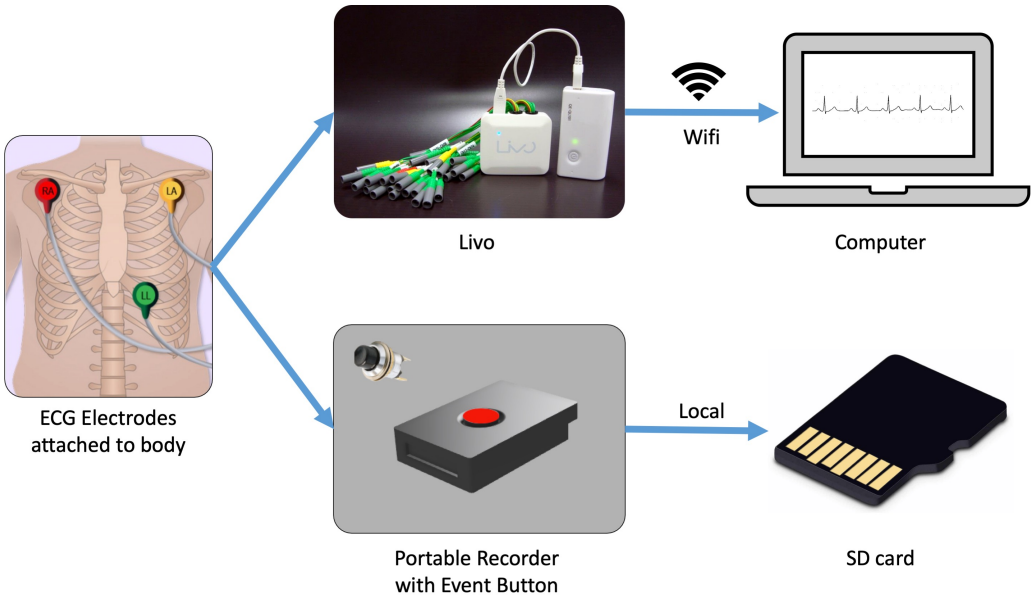

Figure 3.2: Driver biosignal recorders

Data aquisition system

The data acquisition system includes multiple instruments attached to the subject to collect bio-signal data and get driving operation data from the vehicle. The instruments can be divided into 2 subgroups: a cloud-based storage system which allowed multiple separated recording systems can upload and synchronize timestamp with a central computer and local storage including 3 computers collecting data separately. The central computer was connected to the internet through pocket wifi and sent data with its timestamp to the cloud database (Amazon Web Services - AWS). Details of the system are presented in Figure 3.3.

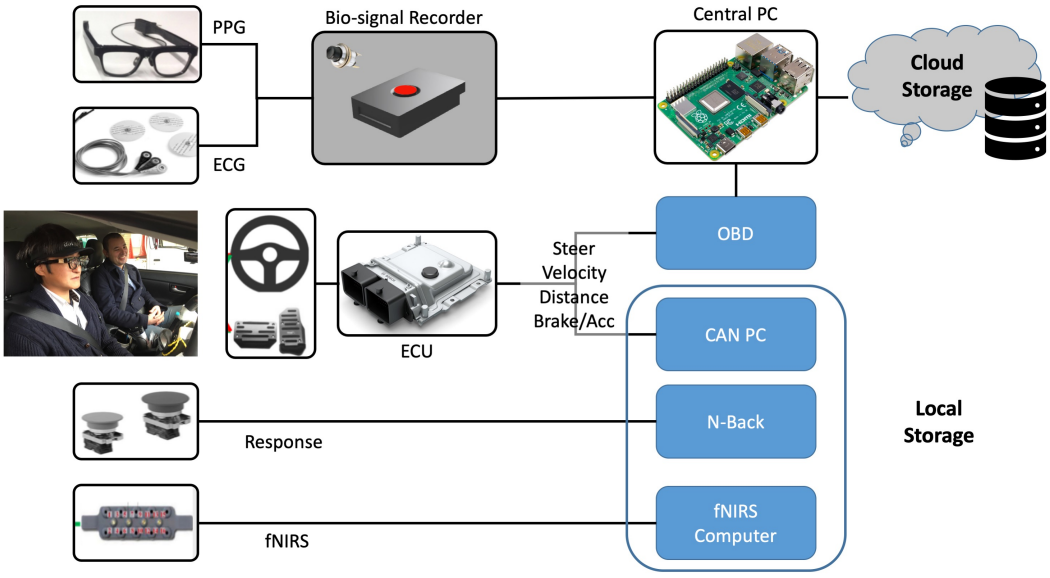

Figure 3.3: Data acquisition system

3.2.3 Driving tasks

The experiment was taken place in the test track of Kyosei driving school, Okazaki city, Japan. The scenarios were designed to evaluate the driving performance and physiological indices under the influence of the complexity of driving and the secondary task.

Primary task

The main task of the subject was to drive and maintain a fixed velocity (autocross) or fixed distance (car following) to the front vehicle on a zigzag line created by pylons on the oval test track. The road of the test track had two lanes with 6 meters width. The distance between 2 pylons is about 50 meters. The pylons were placed near the center line but on the opposite lanes to force the driver to steer in zigzag route. Details of driving task are shown in Figure 3.4

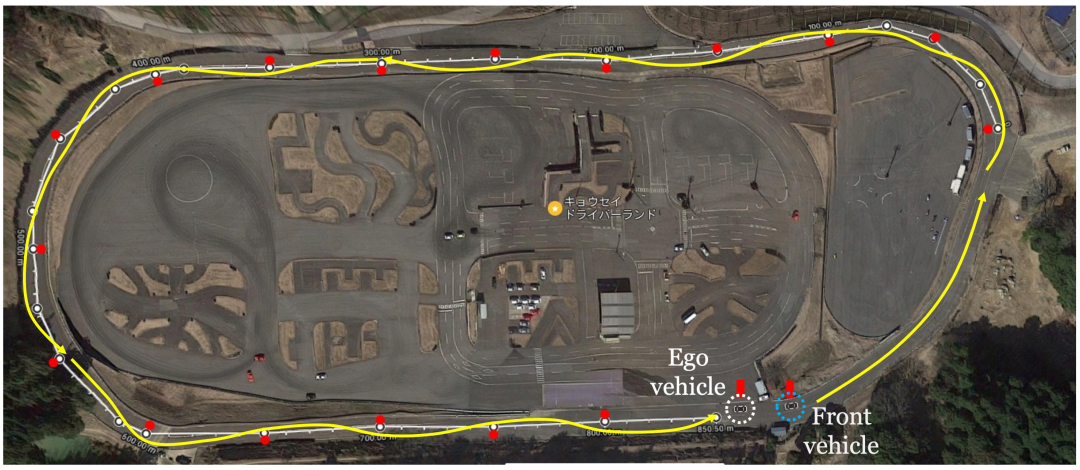

Figure 3.4: Experiment route and driving task

(Course captured from Satellite image of Google Map)

Secondary task

The secondary task was an auditory delayed response number called the n-back task. The task is a type of memory task which require the subject has to listen and remember a series of random number played in a fixed interval. The ”n” in n-back denotes the previous position of the number which the subject has to remember. For example, 1-back means that the subject has to remember the previous number, 2-back means that the subject has to remember the second number to the last one. If the current number and the ”n” number are the same, the subject will press the wright button, otherwise press the wrong button. Figure 3.5 shows an example of 1-back task and 2-back task. Other details of task combination are shown in Figure 3.6.

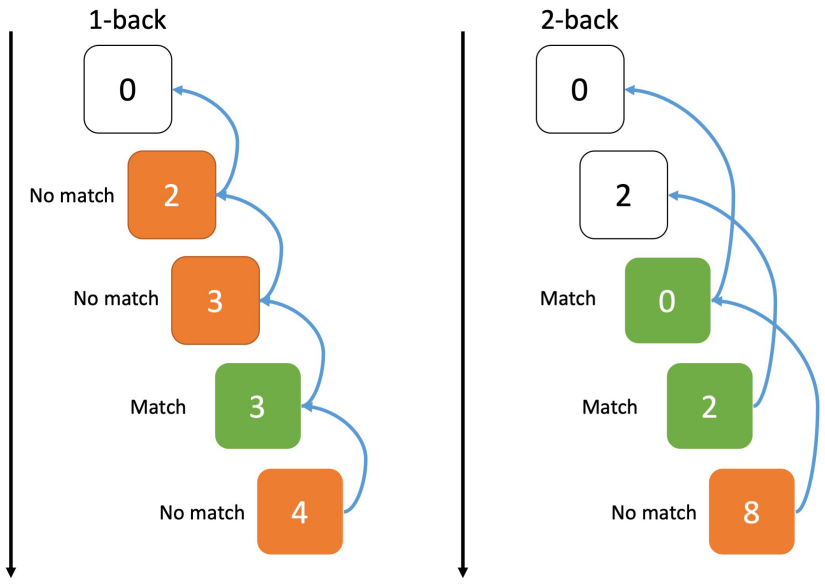

Figure 3.5: Example of n-back task

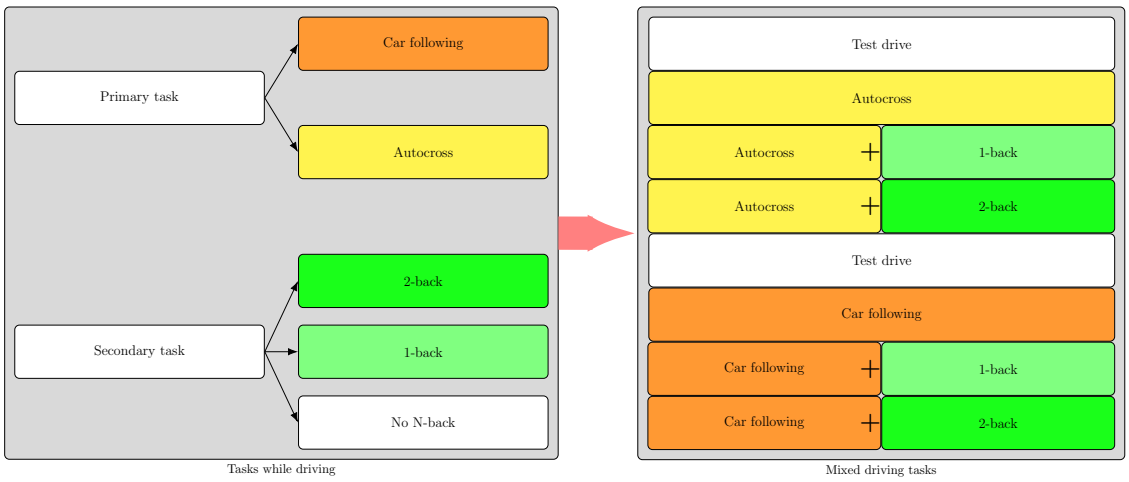

Figure 3.6: Task flowchart

3.3 Results & Analysis

3.3.1 Results

As mentions in the tasks' description, subjects had to maintain either relative constant speed or distance to the front car depend on the type of primary task. Intuitively, comparing the standard deviation of the speed and distance can show the different between normal driving and driving under the mental workload. In real driving on the highway, the cruise control system can detect the distance to the front car. But in this experiment setup, the distance data sometimes cannot detect the front vehicle due to the limit of the detection angle of sensor. As a consequence, the longitudinal parameters used for this analysis is only the standard deviation of the speed and the lateral parameters are the deviation of the steering angle and steering velocity.

As for the ECG data, raw data was extracted and aligned with the driving data by timestamp collected from cloud storage. Extracted data was passed through a median filter to remove the baseline wandering and then passed through a bandpass filter to remove noise (Acharya et al. , 2007). The R-peak detection procedure used a non-linear transformation and first-order Gaussian differentiator technique (Kathirvel et al. , 2011). The procedure was implement in Python code. Figure 3.7 shows ECG data results through the preprocessing: Raw ECG data (top), median filter to remove the baseline wandering (middle), bandpass filter to remove the noise and R-peak detection (bottom). The R-peak outputs then was calculated in Kubios HRV (Tarvainen et al. , 2014) for the HRV parameters. The HRV parameters includes time-series (mean RR-interval, the standard deviation of RR - SDNN) and frequency indices (low frequency - LF, high frequency - HF, LF/HF ratio).

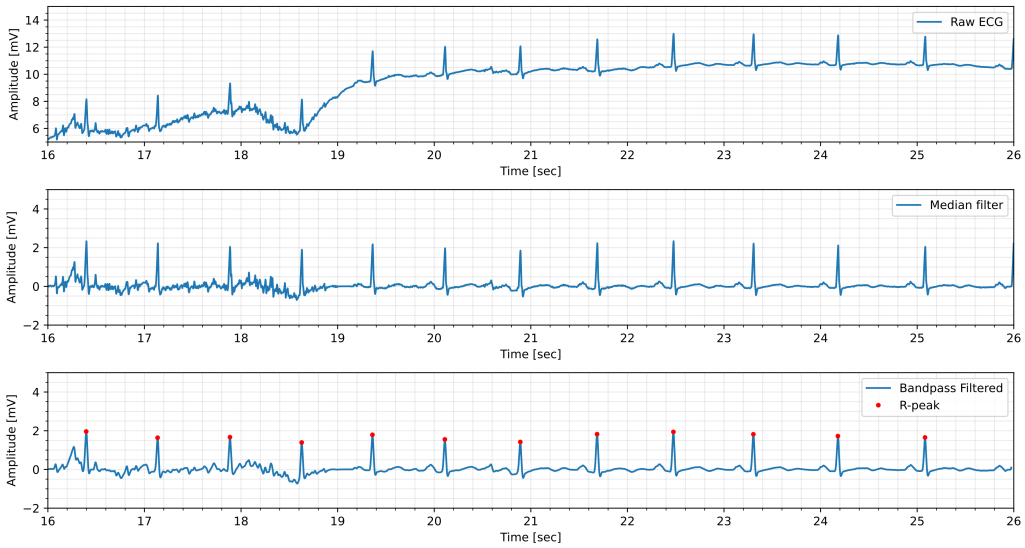

Figure 3.7: Preprocessing ECG data

3.3.2 Factorial analysis

In real-world driving, factors that can affect driver physiological indices and driving performance are immense. Vehicle driving task can be present as demanding of "visual-spatial-ambient + manual resources" (Wickens , 2008). The secondary task which imposes mental workload in this experiment will occupy auditory resource, cognition processing and partially the manual resource. If the two tasks (primary and secondary) utilize the same resources at the same time, the result of the complex task will be less efficient.

Two hypotheses are proposed according to the expected variations of variables in this study:

- *Hypothesis 1:* The types of primary task and secondary task have an effect on the physiological indices and driving performance;
- *Hypothesis 2:* The driver's skill and secondary task have an effect on the physiological indices and driving performance.

3.3.3 Discussion

In general, the driving performances showed no significant difference between the normal driving task and driving with the secondary task except the standard deviation of speed. The detailed results (Figure 3.8-a) showed that in the following task, the standard deviation of speed is higher than the autocross task. While the autocross task results remained fairly stable, the car following showed a decrease when the difficulty of the secondary task increase (no secondary task to n-back task).

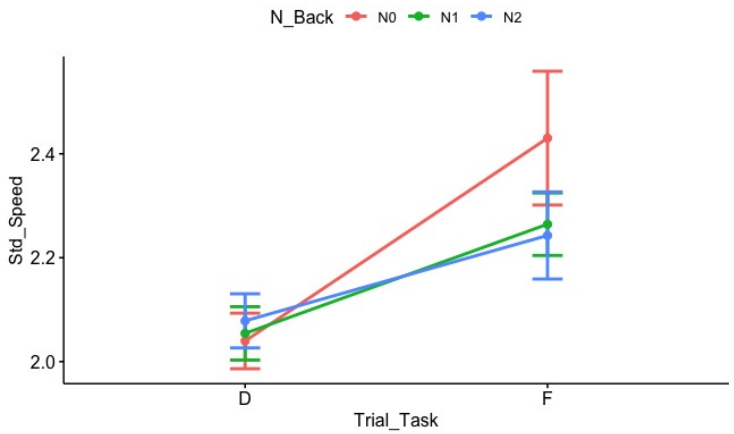

(a) Standard deviation of Speed

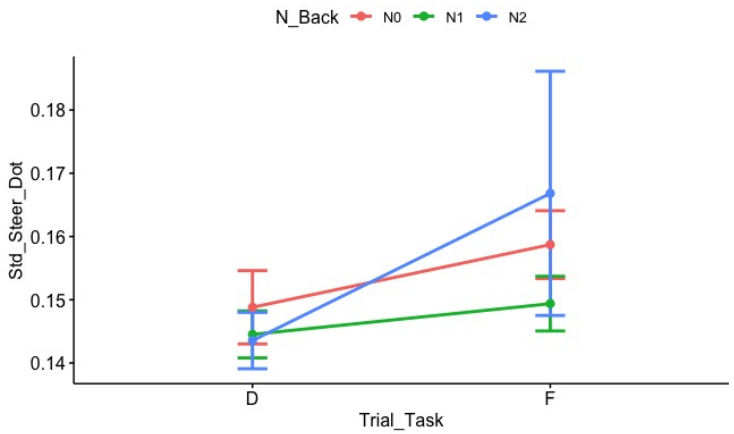

(b) Standard deviation of Steering Velocity

Figure 3.8: Effect of driving task to the driving performance

Primary task: D - Autocross task; F - Following task

Secondary task: N0 - No n-back; N1 - 1-back; N2 - 2-back

The significant difference in the standard deviation of speed (Tabel 3.1) under the effect of driving task might due to the differences of driving without constraining (except maintain speed) and driving with the constrain of the speed and distance to the front vehicle: the driver's mental resource has to share between manual control (driving the vehicle) and visual recognition (maintaining speed and distance).
In case the driver's reaction time increases, the deviation of speed will also increase to maintain the safety condition. This trend also shows in steering performance (Figure 3.8-b). The effectiveness is lesser due to the main requirement of the driving task is longitudinal control. These results show that using driving performance can help clarify the state of driving condition: normal driving and driving while sharing resource for other jobs.
As for the cardiovascular system response, the results indicate that the mental task has a significant effect on the heart-rate (reflected on mean RR) and the standard deviation of heart-rate (reflected on SDNN). In the test of the driving task and n-back task, the n-back task showed a significant effect on SDNN. The result is showed in Figure 3.9 (a). Driver's skill and n-back task had significant effects on both meanRR and SDNN, but showed no effect on the ratio LF/HF (Tabel 3.2).
These results can be explained when considering various factors affect the HRV: age, gender, diseases, life habits, and environments, etc. In general, the mean RR (or mean heart-rate) reflects the physical requirement of the human body. In the resting state, the heart-rate is generally low while the SDNN is high. In the focus state and the physical activities, the sympathetic nervous system prepares the body be ready for the response by increasing heart-rate. Also, the SDNN is lower than the resting state.

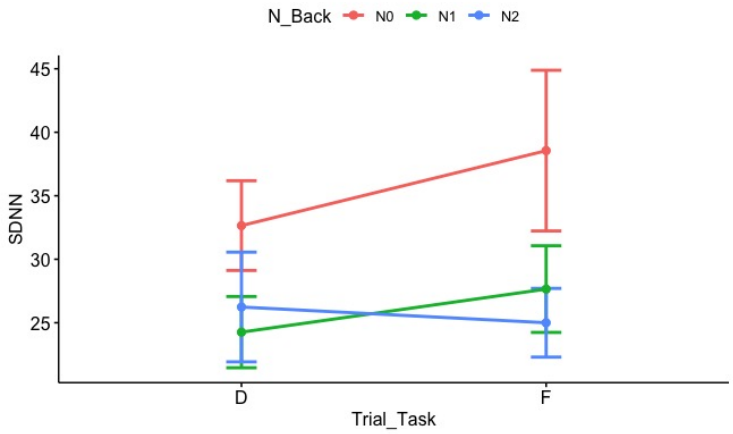

(a) SDNN = Driving + N-back

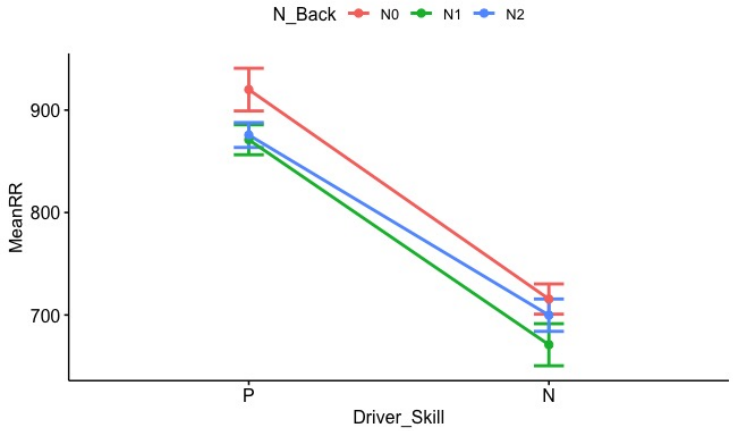

(b) meanRR = DriverSkill + N-back

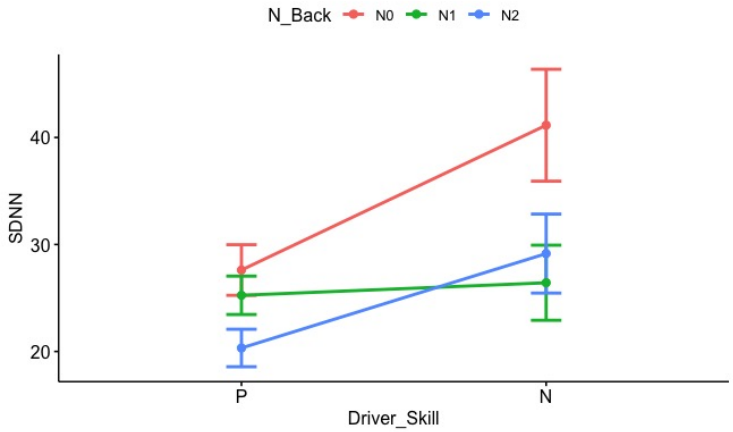

(c) SDNN = DriverSkill + N-back

Figure 3.9: Effects of Driver skill and Tasks to Physiological indices

Primary task: D - Autocross task; F - Following task

Driver skill: P - Professional driver; N - Novice driver

In the driving experiment, the factors which affect HRV reduced are the driving tasks (including types of driving and types of n-back task) and driving experience. As can be seen from Figure 3.9 (b, c), the n-back task induced more stress to the cardiovascular system than normal driving in different levels based on driver's skill.

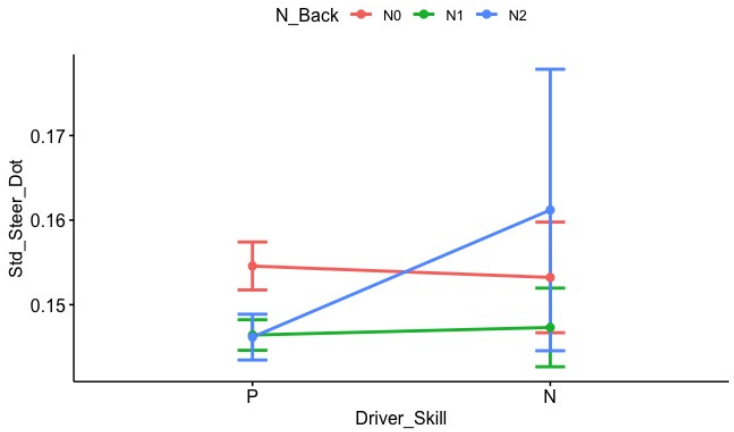

(a)

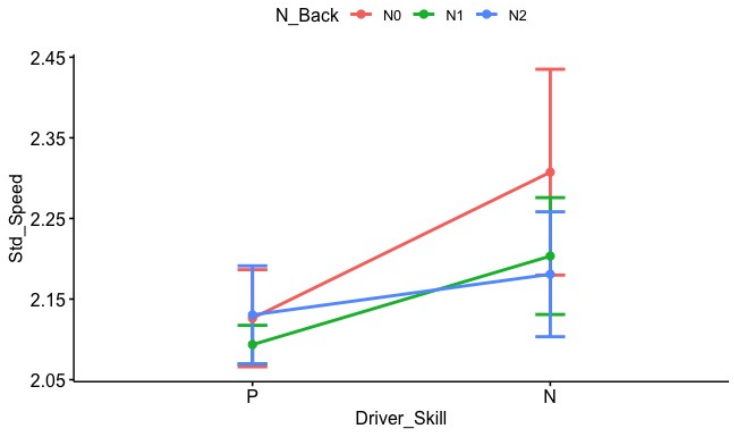

(b)

Figure 3.10: Effects of Driver skill to driving performance

Driver skill: P - Professional driver; N - Novice driver

Secondary task: N0 - No n-back; N1 - 1-back; N2 - 2-back

Another factor should be considered is the characteristics of the individual subjects. All subjects reported that the 2-back task is the most stressful task. While performing the 2-back task, it was too hard for the memory, then the subject just ignored the secondary task and pressing buttons randomly. Since the professional

drivers are more confident about their driving skill, their operations were more gentle and stable than the novice drivers in all tasks, showed as the deviation of speed and steering velocity of professional driver result did not change so much in Figure 3.10. The results of the novice drivers ranges varied larger, especially in case of 2-back, the steering performance of the novice drivers was more erratic (Figure 3.10-a). This result shows consistent with the ANOVA result (Table 3.2) about the driver skill. Driver's experience and characteristics should be taken into account when choosing subjects for future experiment.

Table 3.1: Effects of primary and secondary task

Source	**Sum.Sq**	**df**	**F**	**Pr**	
MeanRR					
Driving task	2.81E+02	1	0.022	8.84E-01	
N-back task	1.78E+04	2	0.684	5.09E-01	
Driving:N-back	9.53E+02	2	0.037	9.64E-01	
SDNN					
Driving task	1.02E+02	1	0.680	4.13E-01	
N-back task	1.22E+03	2	4.076	2.24E-02	*
LF/HF					
Driving task	4.53E+01	1	2.475	1.22E-01	
N-back task	4.18E+01	2	1.142	3.27E-01	
Driving:N-back	3.89E+01	2	1.063	3.53E-01	
Standard deviation of speed					
Driving task	9.75E-01	1	16.516	1.58E-04	***
N-back task	7.49E-02	2	0.634	5.34E-01	
Driving:N-back	1.43E-01	2	1.210	3.06E-01	
Standard deviation of steering angle					
Driving task	2.22E+00	1	0.851	3.60E-01	
N-back task	1.05E+01	2	2.008	1.44E-01	
Driving:N-back	9.92E-01	2	0.1896	0.8278	
Standard deviation of steering velocity					
Driving task	2.41E-03	1	2.9692	9.06E-02	
N-back task	7.75E-04	2	0.4766	6.23E-01	
Driving:N-back	9.06E-04	2	0.5574	5.76E-01	

Note: * p<0.05, ** p<0.01, *** p<0.001

Table 3.2: Effects of driver's skill and secondary task

Source	**Sum.Sq**	**df**	**F**	**Pr**	
MeanRR					
Driver's skill	5.32E+05	1	183.72	<2e-16	***
N-back task	2.13E+04	2	3.677	3.17E-02	*
SDNN					
Driver's skill	8.61E+02	1	6.338	1.48E-02	*
N-back task	1.24E+03	2	4.579	1.45E-02	*
LF/HF					
Driver's skill	1.23E+01	1	0.664	4.19E-01	
N-back task	6.27E+00	2	0.169	8.45E-01	
Skill:N-back	1.48E+01	2	0.398	6.73E-01	
Standard deviation of speed					
Driver's skill	1.58E-01	1	2.087	1.54E-01	***
N-back task	7.00E-03	2	0.043	9.58E-01	
Skill:N-back	4.10E-02	2	0.273	7.62E-01	
Standard deviation of steering angle					
Driver's skill	1.61E+01	1	7.026	1.04E-02	*
N-back task	1.05E+01	2	2.292	1.10E-01	
Standard deviation of steering velocity					
Driver's skill	9.00E-06	1	0.010	9.20E-01	
N-back task	3.66E-04	2	0.215	8.08E-01	
Skill:N-back	9.00E-06	1	0.443	9.20E-01	

Note: * p<0.05, ** p<0.01, *** p<0.001

3.4 Conclusion

In this chapter, the effects of mental workload with the incorporation of other factors to the cardiovascular system and driving performance have been taken into accounted. It can be seen that the heart-rate and the activities of the cardiovascular system in a short time are sensitive to the mental task and driving task. These changes can be used as an indicator to detect different driving states of the driver. The results showed a consistent conclusion with previous research. It needs to process to extend the knowledge to the detection of dangerous states of driving which will lead to accidents.

Chapter 4

Graphical models

4.1 Introduction

Searching for patterns in data has a long history, involving in many fields: statistical analysis, signal processing, image analysis, bioinformatics, computer graphics, etc. Pattern recognition is concerned to automatically discover the regularities of the data and use those finding to take actions such as detection of abnormal data from normal ones or clarifying the data into different categories by utilizing the use of computer algorithms. The key concept is uncertainty. This comes from the noise of the measurements and the limited size of data that can be collected. In the era of big data, the limitation of the data sets can be overcome by employing massive sensors and data sources. The development of computing technology has increase the computational capacity of the machine and open pathways for bigger and bigger models and data sets. As a result, humans have seen the enourmous expansison of the machine learning in the past few decades. The using of deep learning algorithms have help solve a lot of problems with great outcome. But when it comes to the exploration or explanation, those approaches are generally ambiguous. This chapter will introduce an advantaged method to tackle that problems by using diagrammatic representations of probability distributions, *probabilistic graphical models* or in short *graphical models*.

4.2 Graphical models

Graphical models combine the ability to dealing with uncertainty problems through the use of probability theory and an effective approach to handling complexity through the use of graph theory. The application field of graphical models includes chemistry (Bronson et al. , 2010; Olsson and Noé , 2019), genomics (Sinoquet , 2014), neurology (Paz-Linares et al. , 2018; Belilovsky et al. , 2016), psychology (Bhushan et al. , 2019), and social interaction (Zhang et al. , 2010; Farasat et al. , 2015).

Graphical models are graphs which comprise *nodes* (or *vertices*) connected by *edges* (or *links* or *arcs*). Each node represents a random variable and edge represents the probabilistic relationships between these variables. The graph then show the representation of joint probability distributions over all random variables. As for the representation, there are two main kind of graphical models: directed and undirected.

4.2.1 Directed graphical models

In directed graphical models, also known as *Bayesisan Networks*, the edges have a particular direction indicated by arrows. In most of the real-life cases when representing or modeling some event, it would be dealing with many random variables. Even if considering all the random variables to be discrete, there would still be exponentially large number of values in the joint probability distribution. However, many of these variables are marginally or conditionally independent of each other. By exploiting these independencies, it can be reduced the number of values needed to store to represent the joint probability distribution.

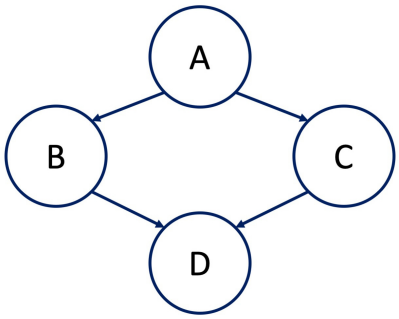

Figure 4.1: A simple directed graphical model

Considering the example in Figure 4.1, the joint probability distribution $p(A, B, C, D)$ across the four random variables A, B, C, and D, by using the chain rule of probability, can be writen the joint distribution in the form:

$$p(A, B, C, D) = p(A) \times p(B|A) \times p(C|A, B) \times p(D|A, B, C) \tag{4.1}$$

By using the conditional independence relationships, the equation 4.1 can be rewritten as:

$$p(A, B, C, D) = p(A) \times p(B|A) \times p(C|A) \times p(D|B, C) \tag{4.2}$$

The terms in equation 4.1, $p(C|A, B)$ is simplified to $p(C|A)$ because C is independent of B given its parent A (denoted as $C \perp\!\!\!\perp B|A$), and $p(D|A, B, C)$ is simplified to $p(D|B, C)$ ($D \perp\!\!\!\perp A|B, C$). The joint distribution of a graph with N nodes can be written in general as:

$$p(x) = \prod_{i=1}^{N} p(x_i|pa_i) \tag{4.3}$$

where pa_i denotes the set of parents of x_i, and $x = x_1, ..., x_N$. This equation expresses the *factorization properties* of the joint distribution for a BN model. Eventhough mentioned above that each node correspond to a single variable, it can be also associated sets of variables and vector-valued variables with the node of a graph. An important restriction to the directed graphs that in the considered graph there

must be *no directed cycles*. In other words there is no closed path (path that one can move from node to node along edges following the direction of arrows and end up at the starting node). These graphs are also called *directed acyclic graphs - DAG*. It can be seen from the example that the conditional independence characteristics allow the graph to represent the joint distribution (equation 4.3) more compactly.

4.2.2 Undirected graphical models

In undirected graphical models, also know as *Markov Random Fields* (MRF), the edges have no directional significance and do not carry arrows. This representation is useful in cases of modeling a variety of phenomena where one cannot naturally ascribe a directionality to the interaction between variables. Undirected models also offer a different and often simpler perspective on directed models, both in terms of the independence structure and the inference task. The edges of *MRF* correspond to some notion of direct probabilistic interaction between neighboring variables. Figure 4.2 shows an example of MRF in image processing.

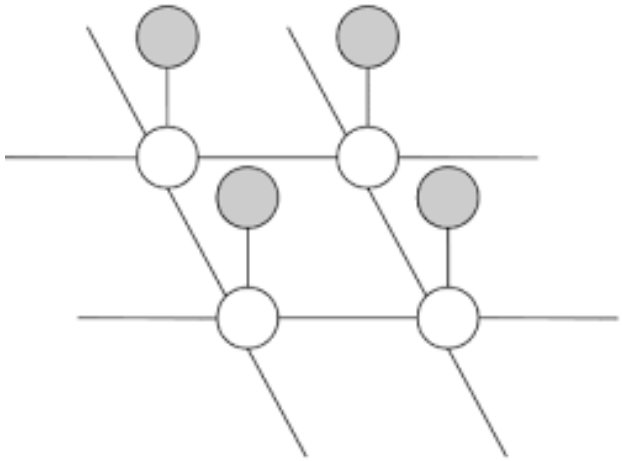

Figure 4.2: An example of undirected graphical model

In the MRF, there is a need to find the *factorization rule* for the conditional independence. Considering two nodes x_i and x_j that are not connected by an edge,

it means that these two nodes are conditional independent given all the other nodes of the graph. This property can be expressed as:

$$p(x_i, x_j|x_{-i,j}) = p(x_i|x_{-i,j}) \times p(x_j|x_{-i,j}) \tag{4.4}$$

where $x_{-i,j}$ denotes the set x with all variables except x_i and x_j. This leads to consider a graphical concept called *clique*, which is defined as as subset of nodes in a graph that there exists an edge between all pairs of nodes in the subset. A *maximum clique* is a clique that cannot be extended by including one more adjacent node. By defining clique, it can be defined the factors in the decomposition of the joint distribution to be the functions of the variables in the cliques. Then the joint distribution of a MRF is defined as follow:

$$p(x) = \frac{1}{Z} \prod_C \psi_C(x_C) \tag{4.5}$$

where C denotes a clique, x_C is the set of variables in that clique, $\psi_C(x_C)$ is the *potential function* on the clique C, and Z is the normalization factor or *partition function* given by:

$$Z = \sum_x \prod_C \psi_C(x_C) \tag{4.6}$$

This factor ensures that the distribution $p(x)$ given by equation 4.5 is normalized. By considering *potential function* $\psi_C(x_C) \geq 0$, it ensures that the distribution $p(x) \geq 0$.

4.2.3 Learning the graph

Learning the graph refers to the structure of the model (topology), or the paramters of the graph, or both. Another important factor in learning the graph is whether all the graph variables are observed or some of them are hidden. This leads to the following ways for classifying learning problems:

- Known structure, full observability
- Known structure, partial observability

- Unknown structure, full observability
- Unknown structure, partial observability

Addition factor needs consideration is whether the goal is to find a "best" model/ a set of parameters, or to return a posterior distribution over models/ parameters. Because the number of graph structures grows exponentially with the number of nodes, it is often nessary to adopt to heuristics to find a good candidate model. Some of the popular methods in learning the graph are the maximum likelihood estimates (MLEs), the estimate maximum a posterori estimates (MAP), the Expectation Maximization (EM), search algorithms, etc.

4.3 Gaussian Graphical Model

The undirected graphs can be divided into subgroups following the correlation condition:

- Marginal Correlation graphs
- Partial Correlation graphs
- Conditional Independence graphs

4.3.1 Marginal Correlation graphs

In a marginal correlation graph, an edge is established between 2 nodes x_i and x_j if a measure of association $|\rho(x_i, x_j)| \geq \epsilon$. Normally, ϵ equals to 0. Sometimes $\rho(x_i, x_j)$ can also be written as $\rho(i, j)$ The parameter $\rho(i, j)$ is required to have the independent property:

$$X \perp\!\!\!\perp Y \; implies \; \rho(X, Y) = 0 \tag{4.7}$$

The measure ρ should have many properties: easy to compute, robuts and there is some way to compute a confidence interval for the parameter. There are some candidates for this measure: Pearson correlation ρ, Kendall τ, distance correlation γ^2, etc.

4.3.2 Partial Correlation graphs

Before looking into the partial correlation graph, it needs to define what is partial correlation. Let $X, Y \in \mathbb{R}$ and Z is a random vector. The partial correlation between X and Y, given Z is a measure of association between X and Y after removing the effect of Z. That means $\rho(X, Y|Z)$ is the correlation between residual e_X and e_Y resulting from the linear regression of X with Z and of Y with Z. In graphical model, let $x = x_1, ..., x_N$ and ρ_{ij} denotes the partial correlation between x_i and x_j

given all the other variables. The matrix of partial correlation $K = \rho_{ij}$ is given by:

$$K_{ij} = -\frac{\Omega_{ij}}{\sqrt{\Omega_{ii}\Omega_{jj}}} \tag{4.8}$$

where $\Omega = \Sigma^{-1}$, Σ is the covariance matrix of x.

4.3.3 Conditional Independence graphs

The conditional independence graph is the strongest type of undirected graph. This means that the edge between 2 nodes i and j is omitted if x_i is independent of x_j given the rest of the variables.

$$x_i \perp\!\!\!\perp x_i \mid rest \tag{4.9}$$

Gaussisan Graphical Models

Considering random vector x is centered and normalized.

$$x \sim \mathbb{N}(0, \Sigma) \tag{4.10}$$

In this case, it goes back to the partial correlation graph. This graph is also called Gausian Graphical Model (GGM).

The partial correlation matrix is often called the *precision matrix*. Equation 4.8 also write as:

$$Cor(x_i, x_j | x_{-ij}) = -\frac{K_{ij}}{\sqrt{K_{ii}}\sqrt{K_{jj}}} \tag{4.11}$$

To represent the GGMs graphically, the partial correlation matrix after being standardized is an asymmetric matrix with the diagonal equals to 1. The off-diagonal elements represent the partial correlation between two 2 elements. Each variable represents a node. If the partial correlation between 2 variables equals to zero, there is no link or edge between them. But this means that the graph is dense. To obtain a sparse model, the partial correlations are forced to zero by using threshold rules.

Figure 4.3 shows an example of representing GGM structure with colored weighted edges.

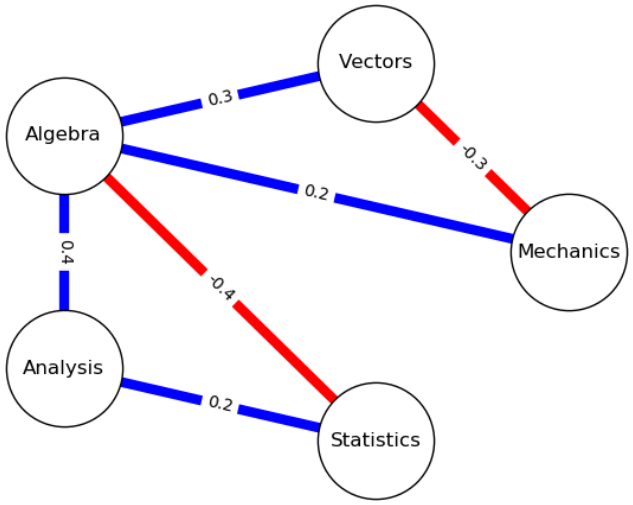

Figure 4.3: An example of GGMs

Interpreting GGMs

The strong point of the graphical model is the capability in exploratory data analysis. In fact many natural phenomena in real life can be approximated by a bell-shaped frequency distribution known as the normal distribution or the Gaussian distribution. This can be used as advantaged when constructing the graph and do the causal interpretation.

According to a review by Epskamp et al. , 2018, interpreting GGMs can be in different ways:

- **Predictive effects**: GGM's edges can be used to show which variables predict another. While using the directed graphs, the interpretation requires a causal inference. While using GGM, for example A-B-C, only information of the middle node (B) is needed when predict the others (A and C);
- **Indicative of causal effects**: eventhough the information of causal is vague in GGMs (the lack of arrows), the exploratory search algorithms perform in

GGMs is easier. Edges in the GGM may be interpreted as potential causal paths;

- **Causal generating model**: the interaction in undirected network models is a two side effect. Link between A-B could be interpreted as intervening on A would impact B, and intervening on B would impact A. This interpretation is useful in discussing the phenomena in psychology, genetics, social networks, etc.

4.4 Conclusion

This chapter has introduced the background of the graphical models. By combining the probability theory and graph theory, graphical model is a powerful tool in solving complex problems with the capability of exploratory. The later part of the chapter breifly bring up the specific Gaussian Graphical Model, how to represent one and the advantages of interpret GGMs over directed graphs.

Chapter 5

Surprise state detection in case of driving misapplication

5.1 Background

5.1.1 Driving misapplication in the world

Startle or surprise responses are quite common in general driving: a sudden obstacle appears, unintended acceleration or lough sound on the road, etc. By definition, startle is a reaction to a sudden, intense threatening stimulus while surprise is inclined toward cognitive and emotional response. These terms are often used interchangeably. In aviation, many studies about their effects on operation functions have been carried out (Rivera et al. , 2014; Landman et al. , 2017; de Boer and Hurts , 2017). In some extreme cases, the surprise may impair the pilot's troubleshooting capabilities. The reaction of road drivers is similar. While subtle surprise events appear more often, more extreme cases such as near hit can develop fear or panic feeling. In a report, Lococo et al. , 2012 stated that startle or panic was common associated with pedal misapplication in the United States. Summary of crash situations and places are shown in Figure 5.1.

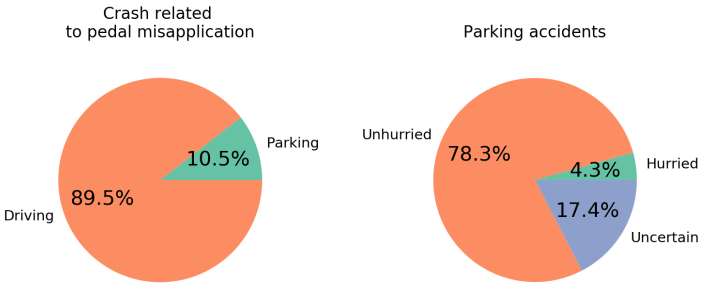

Figure 5.1: Crash locations and situations related to pedal misapplication (data source: Lococo et al. , 2012)

Other studies have investigated the relationship between surprising situations and driving performance. In cases of pedal misapplications, other operation errors might cause unexpected accidents, including human error (wrong direction) and using the wrong gear when starting to drive (Schmidt et al. , 1997). Green , 2000 pointed out that, in unexpected and surprising events, the human perception-brake reaction time increases significantly compared to in fully aware situations (around 0.7-0.75 seconds compared to 1.25-1.50 seconds). Figure 5.2 shows a summary of Green's conclusion about the reaction time. A recent study (Fitch et al. , 2012) also agreed with Green's conclusion that surprised driver responses are slower than those of an aware driver, but these performances vary depending on other factors such as age, gender, vehicle, etc.

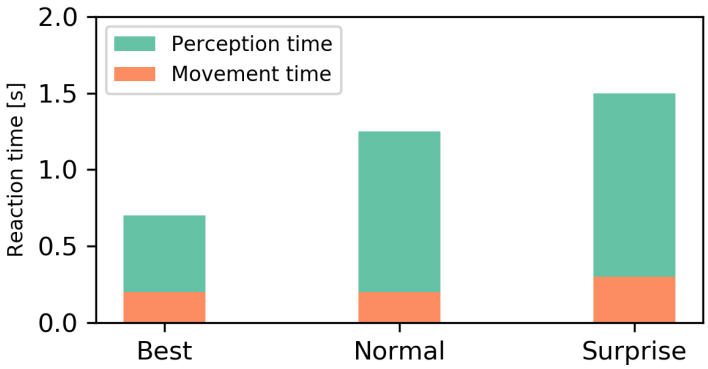

Figure 5.2: Reaction time in driving situations (data source: Green , 2000)

5.1.2 Driving misapplication in Japan

In Japan, the Institute for Traffic Accident Research and Data Analysis (ITRADA) has published reports about driving operation errors and pedal misapplication. As for driving operation errors, drivers aged 24 or under and 75 or over are the groups who cause the highest number of accidents (Masahide , 2014). Figure 5.3 shows an increasing trend of pedal misapplication in elderly groups. Additionally, in Akihiro , 2018 "flustered/panicking" is the most factor common for all operation errors. Figure 5.4 shows the top human factors lead to driving operation errors.

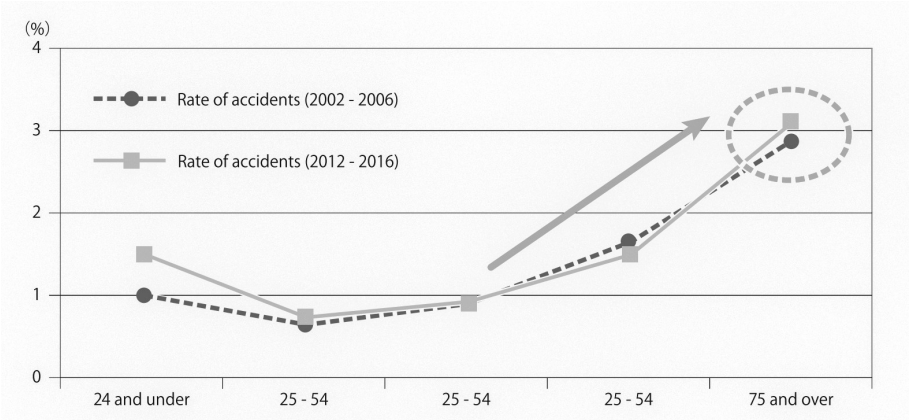

Figure 5.3: Rate of pedal misapplication by age group in Japan

(source: Akihiro , 2018)

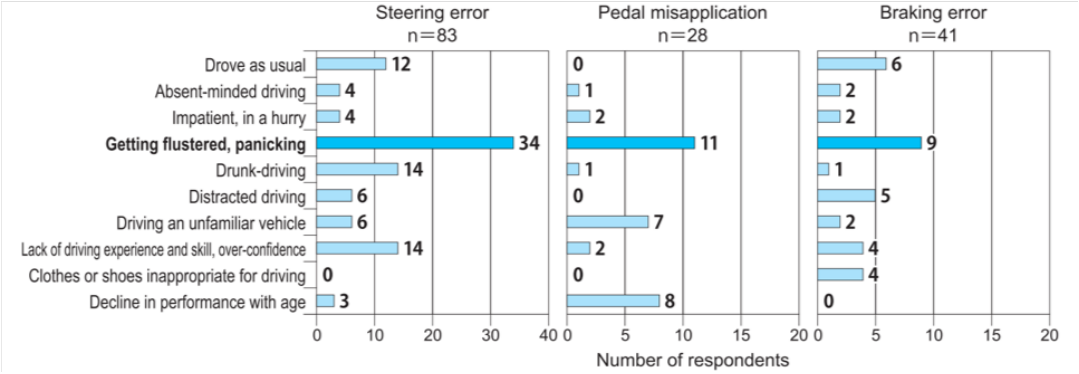

Figure 5.4: Factors lead to driving operation error accidents in Japan

(source: Masahide , 2014)

5.2 Methods

5.2.1 Participants

As mentioned in the previous section, elderly citizens (aged 75 or over) are among the group that causes the highest number of accidents due to operation errors. We conducted a study on 35 participants who participated, with ages from 65 to 85 years old (mean age = 74.3). All have valid driving licenses. The subjects were informed that they must read the instruction and give their consent before they participated in the study. The study was approved by Nagoya University's Institute of Innovation for Future Society Ethical Review Board.

The participants were asked to drive while wearing bio-sensors to collect their biosignal data. Due to the noise in the data (bad contact or loose electrodes) or data corruption, some of the data had to be marked as unusable. The recorder sometimes lost its time system, which led to us being unable to merge the timing between the physiological data and the driving data. Those data were marked as not merged with the driving simulation data. For those above reasons, only 8 subjects' data were used. Figure 5.5 shows the flowchart of data selection.

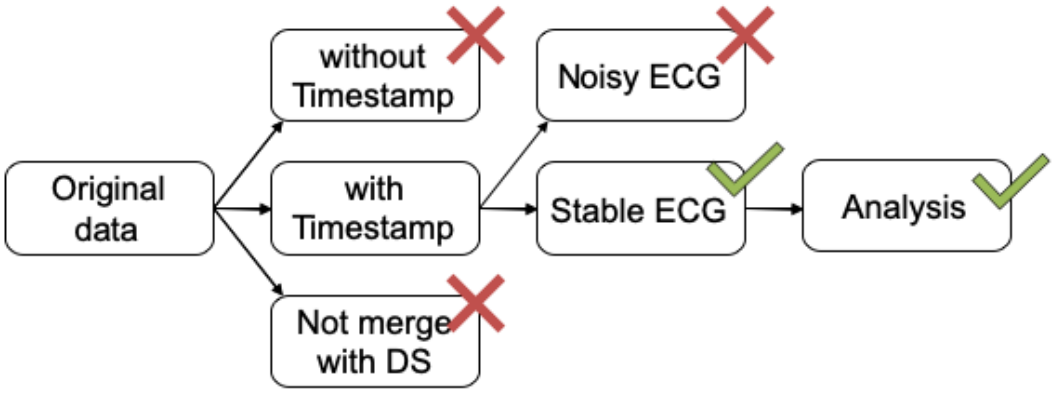

Figure 5.5: Data selection flowchart

5.2.2 Apparatus

Driving simulator

The surprising situations are exposed to high risk of accidents. In order to ensure the safety of the participants, the experiments were conducted in an advanced simulation room in the NIC Building, Institute of Innovation for Future Society, Nagoya University. The simulator was a 5-screen 4K projectors with a stereoscopic-view driving simulator incorporates with many other elements such as: traffic simulation, and vehicle dynamics and performance, by building upon the UC-win/Road software (FORUM8 Co. Ltd.).

- Projectors:
  - Support 4K, 120 Hz, 3D Active stereo for Front, Left, Right and Floor screens
  - Support Full HD for Back screen
- Screen size: W 5400 mm x H 2850 mm

The logging function of UC-win/Road recorded the driver's operation and the vehicle's dynamic values. The logging data is recorded to the log file for latter analysis or can transmit in real-time through the UDP connection other interaction with the system. The trigger condition for the alert was also received through the UDP connection. As mentioned before, the system can provide a lot of information related to the operation and vehicle dynamics. The manual of UC-win/Road has the comprehensive detailed and description of the parameters. Table 5.1 only lists some of the parameters.

Table 5.1: List of parameters can be acquired from Driving simulator

Parameter	**Unit**	**Range**	**Description**
position X	meter	East +X	Position of the vehicle
position Y	meter	Up +Y	same as above
position Z	meter	North +Z	same as above
Yaw angle	radian	South = 0	Yaw angle of the vehicle (Counter clockwise)
Pitch angle	radian	Horizonal = 0	Pitch angle of the vehicle (Up = positive rotation)
Roll angle	radian	Horizonal = 0	Roll angle of the vehicle (Right inclination = positive rotation)
speedInMetresPerSecond	m/s		Velocity of the vehicle
steering	ratio	[-1..+1]	Input on the steering wheel (-1: Max left, +1: Max right)
steeringVelocity	1/s		Rotation rate of the steering wheel
throttle	ratio	[0..+1]	Input on the gas pedal (0: Release, +1: Full throttle)
brake	ratio	[0..+1]	Input on the brake pedal (0: Release, +1: Full brake)

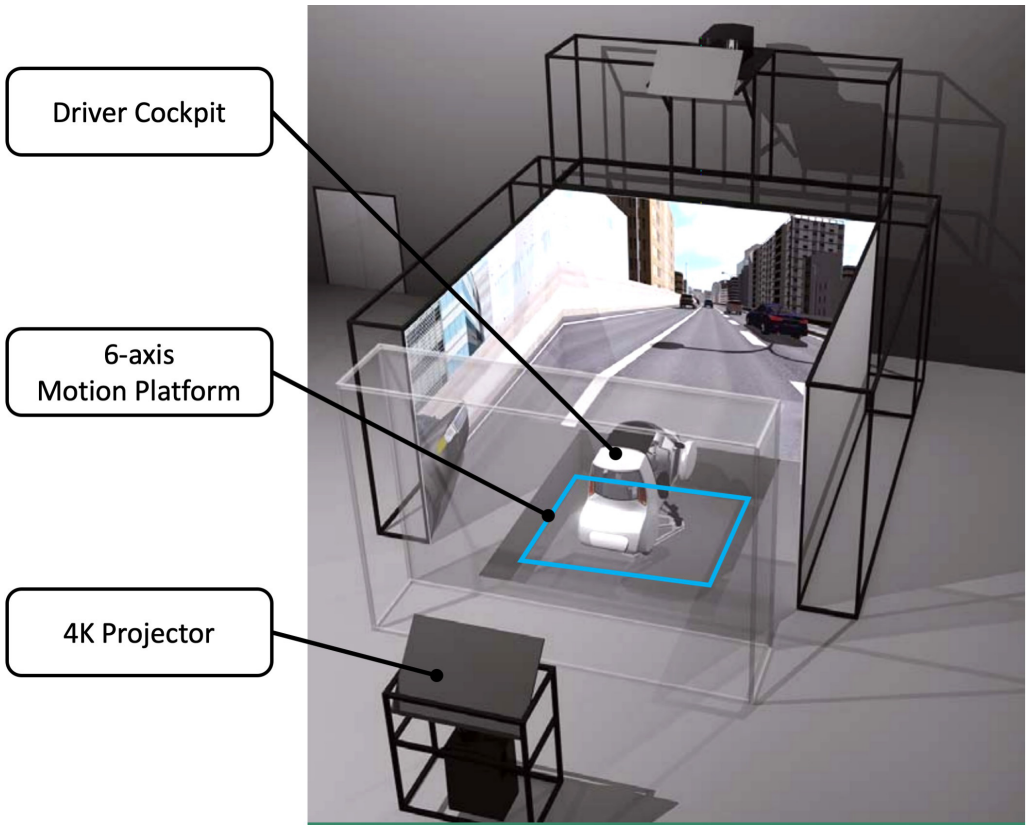

Figure 5.6: Overview of Driving simulator system

Figure 5.6 shows an overview of the driving simulator room. To provide additional information besides driving information,monitoring cameras equipped inside the cockpit to monitor driver operation (behind), face expression and posture (front), and foot movement (over the feet compartment). The recording videos were synchronized with the UC-win/Road time system. Figure 5.7 shows the images captured during the experiment.

Figure 5.7: Camera capture images inside the cockpit

Human machine interface

To investigate the effectiveness of different alert types, there was a human-machine interface (HMI) system alerted the driver about the dangerous distance between the vehicle and the obstacle. The system consisted of a screen put on the instrumental dashboard in front of the driver, a speaker put under the driver seat, and a vibration motor put under the brake pedal. Upon receiving a warning signal about the distance, the HMI system will alert the driver with one of a combination of 4 types of warning — a message on the display, a high-pitched warning sound, a human warning voice, and a vibration — named pattern 0 (P0) to pattern 6 (P6). Details of the alert patterns and descriptions are showed in Table 5.2

Table 5.2: Alert patterns used in the experiments

Pattern	Display	Buzzer	Voice	Vibration	Description
P0	-	-	-	-	Driving without any alert
P2	◯	◯	◯	-	When triggered, display flashing, buzzer gives alarm, and a guidance voice
P3	-	◯	◯	-	When triggered, buzzer gives alarm and a guidance voice
P4	◯	◯	-	-	When triggered, display flashing and buzzer gives alarm
P5	-	-	◯	◯	When triggered, vibration at the acceleration pedal and a guidance voice
P6	◯	◯	-	-	When triggered, the integrated device (display and buzzer) turns on display and alarm

Physiological data recorder

Physiological data were recorded by the same portable recorder used in Chapter 3. ECG recordings used a lead II configuration at a sample rate of 1000 Hz. Depending on the subject's medical history, isopropyl alcohol or non-alcohol cleaner were used to clean the skin and standard pre-gelled disposable electrodes (Ag/AgCl paste,

Vitrode Bs-150) were applied. The recorder did not have an internal real-time clock, so the time system was synchronized with the UC-win/Road time system through the wireless network. The bio-signal was recorded continuously without interruption, and the experiment events were marked by a button event operated by a monitoring operator seating behind the driver seat.

5.2.3 Driving tasks

The tasks were designed to evaluate various driver internal response and reaction to the surprising situation and alarm sources. Figure 5.8 shows the overview of the scenario and the task areas.

Designated tasks

- **The first task** was a trial drive which allowed the subjects to become familiar with the driving environment. In this task, the driver would drive through a straight road and pass a bus stop in the same lane, which required the driver to slow down and change lane. This setup helped the subjects to become used to the feeling of driving with the simulator system. This task was conducted on the "Trial driving" area shown in Figure 5.8. Because the subjects drove as instructed and some subjects felt nervous, the data variation of the first task was large and excluded in the analysis of this research;

- **The second task** was to drive through an intersection with traffic control and then drive into a parking lot in front of a food court;

- **The third task** was the main focus of this experiment, which was to create a surprising scenario. At the parking lot, the subject was asked to move out; the gear shift was intentionally reversed by the operator, causing the vehicle to move toward to the food court instead of moving backward. The second

task and third task were conducted on the "Driving & Parking" area shown in Figure 5.8.

After the first task, the subjects were asked whether they felt comfortable with the driving conditions and whether they could continue with the experiment. The second task and third task were carried out continuously without a break. The subjects were informed about the overall objective of the experiment but were not told when the surprise event would occur. The task sequence was carried out in an orderly fashion by the operator. To prevent any negative influence on the driving state, the subjects were asked to take 5 minutes resting before starting the test. The subjects were asked to drive in their normal driving style.

Normal driving

The normal driving state was considered to be all the data collected throughout the normal driving situations, including the second task (driving along the street) and part of the third task (before the surprise event).

Surprise state

The surprise state was considered to be the data recorded in the latter part of the third task, when the subject reacted to the unexpected movement. Because the subjects expected to move backward but instead moved forward toward the store in front of where they were parked. Some drivers could realize the situation, release the gas pedal and press the brake pedal in time; other could not realize or could not react fast enough and hit to the wall in front of the vehicle. This setup was considered a surprising event.

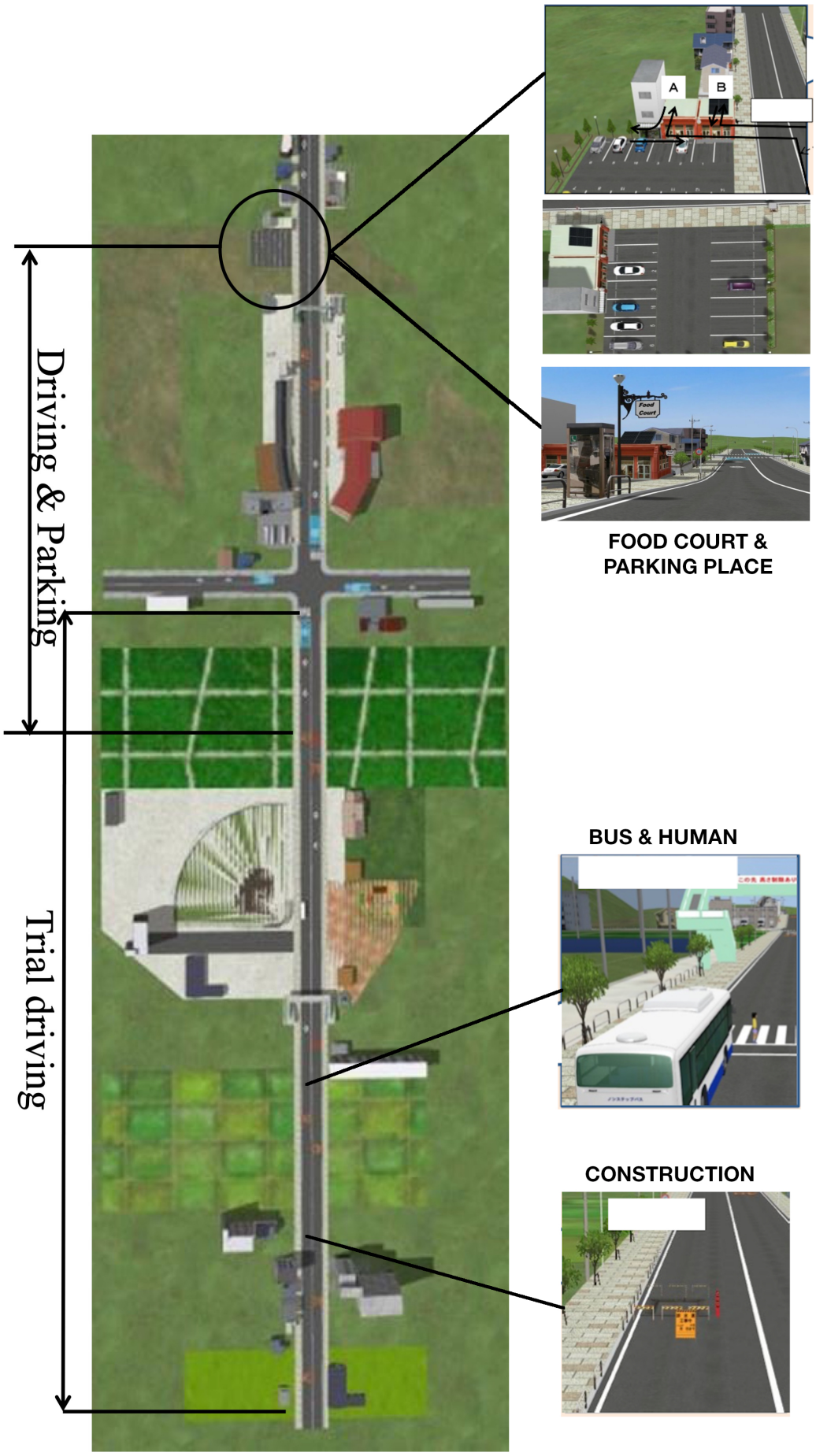

Figure 5.8: Driving scenario and tasks

Besides the human factors and driving performance, the effectiveness of the alert source in the last task (reverse gear) was taken into consideration to improve the driver's reaction. To keep the surprise feeling intact, each subject only experimented once with one of the six alert patterns. The subjects were not informed about the alert pattern before it happened and were asked about their awareness of the alert after the test. Other details of the experimental setup was presented in Tsujita et al. , 2019.

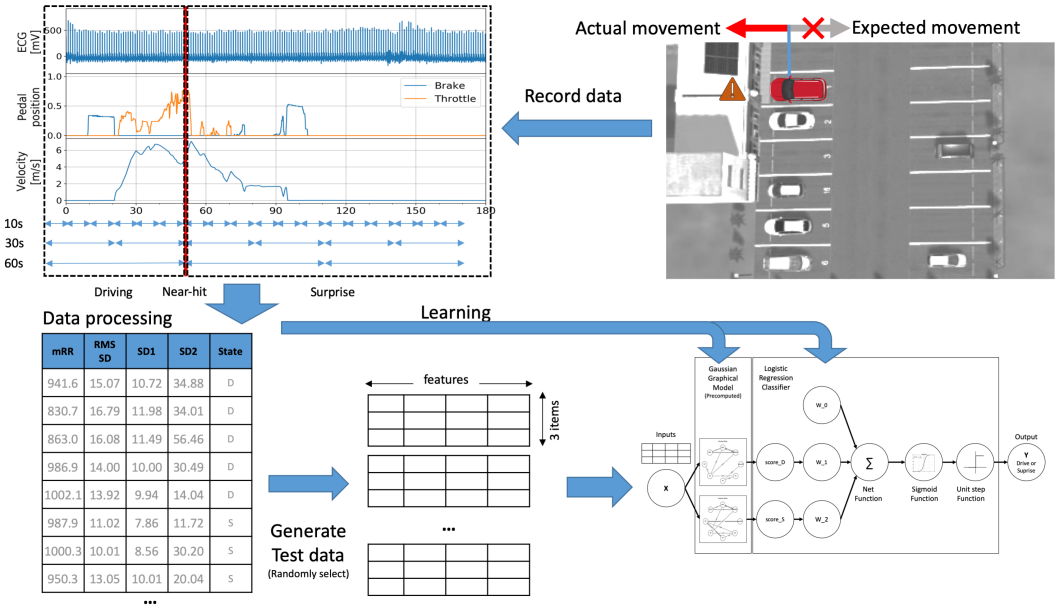

Figure 5.9: Data collection and Model training procedure

5.3 Input data

Physiological data

The physiological features using in this study is the cardiac information, specifically heart rate and HRV indices. The raw ECG data went through the same preprocessing procedure in Chapter 3: a noise filter and extract RR interval. Then, the processed data were divided into windows (10 seconds, 30 seconds, 60 seconds). The window sizes were all under 5 minutes, they were considered to be an ultra-short analysis of HRV. According Pecchia et al. , 2018, the features which are used for investigation for an extremely short period of RR series are the mean RR, RMSSD, LF, HF, and SD1 & SD2. The meaning of each feature depends on the nature of the statistical index. To ensure the integrity of the study only mean RR, RMSSD, SD1, and SD2 were used as input data for the investigation.

5.3.1 Driving information

As for the driving-based information, the driving scenario focused on the longitudinal dynamics of the vehicle, the driver's reaction to the driving scenes, and the safety evaluation of the outcome. In this experiment, only the reaction time during the transition between the acceleration pedal and the brake pedal was considered. The reaction time could only be calculated in a specific period due to the discrete nature of the pedal operation. While driving, some drivers used the brake pedal more often, and others prefer releasing the gas pedal to slow down and only fully stop in case of stopping. Thus, for a short time (in 10 and 30-second windows) some of the extracted data had no reaction operation and the extracted data was null. As a result, the representative RT feature was extracted and used only in a 60-second window analysis.

5.4 Graphical-based detection model

The graphical-based model combines two layers: a layer of GGM and a layer of Logistic Regression Classifier were put into a sequence. Following the assumption of the GGM, all inputs (features) needed to be standardized. In the learning phase, the driving data were used to estimate Driving GGM, and the surprise data were used to estimate Surprise GGM. The labeled inputs were grouped, and we used QuickGraphicLasso method from "skggm: Gaussian graphical models using the scikit-learn API" (Laska and Narayan , 2017) to estimate the respective GGM models. To reduce the uncertainty of estimate the undirected graph, model selection method was used, specifically in this study was the cross-validation. The initialization also affected the outcome of the model, so that different random seeds were tested and chose the best result.

The objective of the model was to combine HRV indexes, reaction time, and alert patterns to classify the driver's state . By using the structures acquired from GGMs, the relationship between these inputs with structural changes in the models can explain the influences of one node (feature) to another. As explained in Driving information section, only 60-second windows had the reaction time data, and thus these data were used in the model. The model inputs include: meanRR, RMSSD, SD1, SD2, alert type, and reaction time. Because the number of input data was small, all data sample was used for the learning phase.

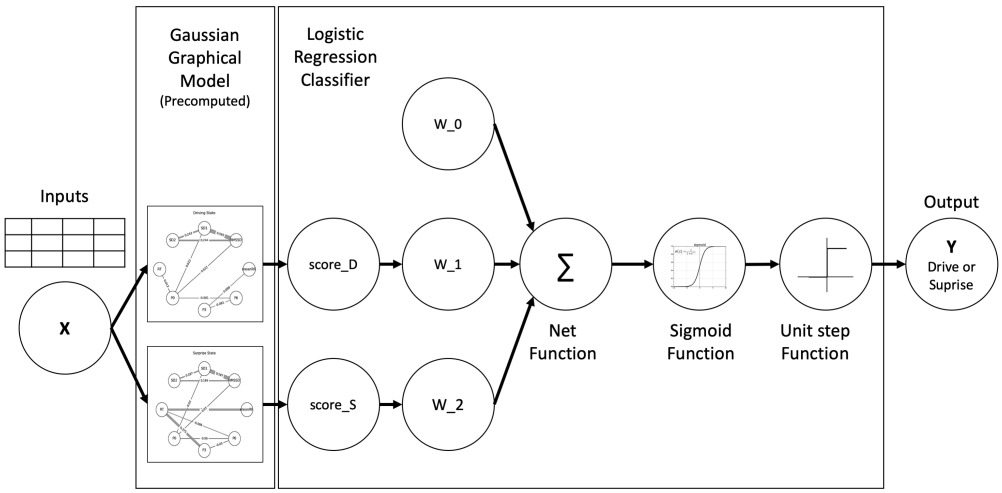

Figure 5.10: Proposed model

The trial data is presented in the same form with the input data

$$Z = \{Z_1, \ldots, Z_p\} \tag{5.1}$$

The sampled data contained p features x m, where m is the length of time. Assume that the trial data belongs to one of the GGM models discussed above, the score function is used to test which model fit the trial data. The score function is the log-likelihood value of the covariance of the Gaussian trial data with the covariance of the estimate graph model. This value is used to represent how "likely" the test data belong to the graph model. The training trial data are extracted by a segmentation data set, as shown in Figure 5.9. Since the data set was small, synthetic test trial data were created to test the performance of the detection method. The test trial data were randomly selected from the data set by the group labels "Drive data" and "Surprise data". The test trial data were then labeled according to their group.

Then the score values obtained by the precomputed GGMs were used as the input of the Logistic Regression Classifier. The Logistic Regression Classifier was trained by the train trial data. The detailed structure of the graphical detection method is shown in Figure 5.10.

5.5 Results analysis

5.5.1 Basic statistical result

Table 5.3: Mean and SD of the heart activites and reaction time

	Normal state		Surprise state		Unit
Variable	Mean	SD	Mean	SD	
RR interval	911.3	64.5	934.7	55.2	ms
Heart-rate	66.3	4.5	64.6	3.8	bpm
Reaction time	1792.4	286.3	463.8	129	ms

Tabel 5.3 shows that the mean of HR in the surprise was lower than the mean of HR in normal driving. This change is somewhat unexpected as typically one would assume that the heart rate should increase as a response to a surprise event. In most of the case the cardiac activities increase right after the stressful event then gradually decrease back to normal. Nomikos et al. , 1968 mentioned that cardiac acceleration or deceleration was due to individual differences. Gantiva et al. , 2019 reported about the psychological responses to facial expression in which the image sudden appeared, the HR decrease and startle reflexes increase indicated that the rising of attention response and preparation for "fight-or-flight" response of the SNS system.

5.5.2 Cannonical machine learning methods

In order to evaluate the performance of the proposed model, three canonical classification models were trialed in this study due to their popularity in small data

sets: support vector machine (SVM), random forest (RF), and multilayer perceptron (MLP).

As mentioned in Section 5.3, the input data were segmented into time windows of 10 seconds, 30 seconds, and 60 seconds to create three data sets. Due to the limit of the sample size, the data set extracted with the 60-second time window was excluded in this section and only used with the proposed model.

The data sets were then divided into training sets and test sets to evaluate the performance of the conventional machine learning models. The division ratio was 80:20. The preprocessing, learning, prediction, and cross-validation were carried out using the APIs of scikit-learn (Pedregosa et al. , 2011) in Python.

Due to the limitation of the collected data, the number of surprise state data was significantly lower than the number of drive data. The imbalance of the data will have affected the performance of the model. For that reason, the synthetic minority over-sampling technique (SMOTE) (Chawla et al. , 2011) was used to balance the number of two classes.

Overall, the accuracy of RF was the best among the canonical methods (0.98-0.99 in the training set, 0.71 in the test set). The accuracy of SVM and MLP were a little better than those of a random guess (0.64-0.65 in the training set, 0.48-0.50 in the test set). Other indexes reflecting the effectiveness of the models (Precision, Recall, and F1-score) are shown in Table 2.

Table 5.4: Performance of SVM, RF, MLP, and the graphical model

Model	Window size (sec)	Num. of Samples	Acc. on train set	Acc. on test set	Precision	Recall	F1-score
SVM	10	278	0.65	0.48	0.58	0.54	0.56
	30	95	0.65	0.50	0.50	0.43	0.46
RF	10	278	0.99	0.71	0.85	0.63	0.72
	30	95	0.98	0.71	0.88	0.50	0.64
MLP	10	278	0.64	0.48	0.58	0.52	0.55
	30	95	0.64	0.50	0.50	0.36	0.42
GGM-L	10	278	0.73	0.57	0.77	0.21	0.32
	30	95	0.67	0.59	1.00	0.18	0.31
	60[1]	48	0.80	0.66	0.77	0.47	0.58
	60[2]	48	0.94	0.94	0.94	0.97	0.96

[1] without RT [2] with RT

5.5.3 Graphical-based methods

The performance of the proposed graphical model was shown to be favorable in the case of the 60-second data set with RT information. In the case of the 60-second data set without RT, it was also better than that of SVM and MLP.

5.6 Discussion

5.6.1 Machine learning methods

Among the trialed machine learning methods, RF had the highest accuracy (in both the training set and test set). The gap between the training and test accuracy might be the effect of overfitting. The cross-validation and model selection method could reduce this phenomenon.The high precision shows that the model used in this study is good at detecting the surprise state. However, the low recall reflects that the model is bad at detecting the driving state and tends to mistake the driving state for the surprise state. This might be the effect of the synthetic data creation by SMOTE to balance the data. In this study, those machine learning methods were also tested without SMOTE. Even though the accuracies were better but the performance indexes were worst.

The limited sample size has significant effects on the performance of the machine learning methods, especially MLP did not converge during the training. It can be seen that the performance indexes of SVM and MLP decrease correlated with the decrease of sample size.

The surprise state in driving involves not only the cognitive function but also the sensorimotor function (bodily movement, steering, and leg movement). Using only physiological measures will not be as effective as the addition of other information on driver behavior and the driving context in detecting driver states under varying external conditions. Similar results have been found by other studies (Solovey et al. , 2014; McDonald et al. , 2020).

5.6.2 Graphical-based methods

Despite the fact of limited sample data, the proposed model yield the best performance in detecting driver state compared to the other machine learning

methods. In reality, the number of usable data points for human behavior in driving is limited. The performance of the model with a small data set is an advantage. Further more overcome the limitation of sample data will be considered as future work.

Another important factor when using graphical models is inference. The two graphical models (GGM for driving state and GGM for surprise state) included in the learning phase have the same features (nodes). Because the driver states for each model are different, two models were acquired with different structures. The changes in structure will lead to a better understanding of the interaction between the models' features.

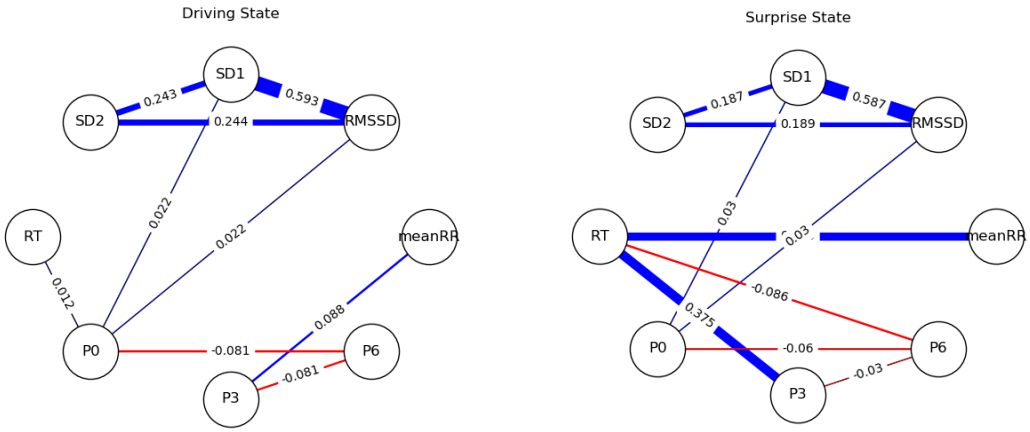

Figure 5.11: Graphical structures for (Left) driving state and (Right) surprise state

Figure 5.11 shows the results of the two models estimated from the data. The changes in the structure of those two models can be seen clearly.

Drive state

In case of the drive state, reaction time has almost no relationship with the other features. The partial correlation with P0 (no alert) is very small, which is under-

standable because there is no alert source to affect other human factors.

Surprise state

The changes in the model structure of the surprise state are noticeable. The partial correlation between the pair "RT - mean RR" and "RT – P3" is positive. The partial correlation of the pair "RT – P6" is negative. There are little changes in the partial correlation between the nodes SD1, SD2, and RMSSD and the other nodes. These results can be interpreted as meaning that the reaction time and the inner system have less influence in normal driving, though in a surprising situation they interact with each other closely.

Effectiveness of alert type

The interesting point here is that the alert type also affects the reaction time but in an opposite way. P3 and P6 use a similar alert source—auditory (voice in P3 and alarm in P6) and visual (display in both patterns). But P3 tends to have a positive influence on RT while P6 tends to have a negative effect. This phenomena can be interpreted as the alarm (P6) reducing the RT. Conversely, the voice (P3) tends to prolong the RT. It can be inferred that the human sensing system and brain respond in different ways to the alert sources. As a result, the human sound appears to be effective in the case of giving instructions, such as in take-overs (Forster et al. , 2017). On the other hand, the response to the alarm takes less time; the human brain can automatically acknowledge the serious problem and take action in a shorter period (Kozak et al. , 2006; Campbell et al. , 2007). The questionnaire result also showed that the alarm sound was more effective than the other warning sources.

5.7 Conclusion

This chapter has investigated different detection methods for surprise state in driving. The graphical-based detection model shows a good potential in both the prediction performance and exploratory inference ability. Although there is a limitation in the data samples, the result show that it was consistent with those of previous studies. The favorable outcome also shows that this approach can be applied not only to this specific case but also to other human behavior that need to have deeper knowledge of the internal interaction.

Chapter 6

Drowsiness detection in driving

6.1 Background

Drowsiness (or Sleepiness or Somnolence) is a state of strong desire for sleep. Sleepiness associated with the low level of arousal which is a serious cause of traffic accidents. The naturalistic driving study found that drowsy driving contributed to 22%–24% of the crashes and near-crashes observed (Klauer et al. , 2006). The other crash survey data showed that this problem is not a specific problem of the United States. The survey conducted by the European Sleep Research Society showed that the median prevalence of sleep-related accidents was 7.0% among 19 European countries(Gonçalves et al. , 2015). The rate of falling asleep on the wheel in Tokyo (Japan) is higher to 10.4% (Komada et al. , 2010).

The stages of sleep can be categorized as awake, non-rapid eye movement sleep (NREM), and rapid eye movement sleep (REM). The dangers of drowsiness come from the second stage, NREM. NREM can be subdivided into three following stages:

- **Stage I**: the transition from awake to asleep (drowsy)
- Stage II: light sleep
- Stage III: deep sleep

6.2 Experiment setup

6.2.1 Participants

There are 11 participants (7 males, 4 females, aged from 30 to 65) in this study. All have valid driving licenses. The subjects were informed the instruction of how to maintain awake state and sleepiness state before they participated in the study. The study was approved by Nagoya University's Institute of Innovation for Future Society Ethical Review Board.

6.2.2 Apparatus

Driving simulator

Due to the high risk of driving in the drowsy state, the experiments were conducted by using a simulator putting inside a dark and quiet room in the NIC Building, Institute of Innovation for Future Society, Nagoya University. The driving scene was created by the UC-win/Road software (FORUM8 Co. Ltd.). The logging function of UC-win/Road recorded the driver's operation and the vehicle's dynamic values. System configuration is shown in Figure 6.1.

Driver biosignal recorder

Physiological data were recorded by the same portable recorder used in Chapter 3 and Chapter 5. ECG recordings used a lead II configuration at a sample rate of 1000 Hz. Isopropyl alcohol cleaners were used to clean the skin and standard pre-gelled disposable electrodes (Ag/AgCl paste, Vitrode Bs-150) were applied. The biosignal was recorded continuously without interruption, and the beginning and the end events were marked by a button event operated by the system operator.

6.2.3 Driving tasks

There were two types of driving in this experiment: awake driving and sleepiness driving. Subjects were asked to drive the same 8-shape highway road in total around 12 minutes (Awake driving) and 24 minutes (Sleepiness driving) one time. The vehicle will try to follow a front vehicle with constant speed (80 km/h) without any restriction.

- **Awake driving**: the participants were asked to maintain their normal sleep routine, recommend to sleep at least 6 hours per day;
- **Sleepiness driving**: the participants were asked to restrict sleeping time in two consecutive days (sleep time maintains around 3-4 hours per day) and cannot drink any coffee on the experiment day.

On the experiment day, the participants were asked to answers questionnaires include a sleepiness scale to confirm their sleepiness states.

Figure 6.1: Experimental setup

Driver camera

A camera device for face detection was also used to record the driver reaction in the dark room. The camera brand is OMRON camera. This camera has the ability to record video in low light environment and detect the face at the speed of 30 frames per second. The videos acquired from the camera will be labeled by 2 operators individually to confirm the driver state based on NEDO drowsiness level

Table 6.1: NEDO drowsiness level

Level	Definition	Symptoms
0	Awake	Fully awake
1	Some what	Show some symptoms of tired
2	Neither sleepy nor awake	Symptoms of tired, sleepy more often
3	Sleepy	Yawn, sometimes close eye
4	Very sleepy	Take effort to state awake
5	Almost fall asleep	Sometimes fall asleep

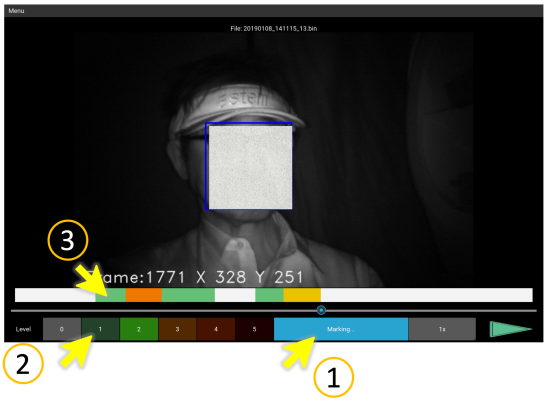

Figure 6.2: Video marker by operator

1 - Status; 2 - Drowsiness level; 3 - Drowsiness making

6.3 Detection methods

Sleepiness evaluation methods can be divided by what is measured (sleep propensity or somnolence) and the nature of the method itself: objective measurement or subjective measurement method.

Sleep propensity

In sleep propensity methods, the test is used to measure either the amount of time taken to fall asleep or the ability to remain awake when instructed. Two famous tests for sleep propensity are the multiple sleep latency test (MSLT) and the maintenance of wakefulness test (MWT). Both tests require using sleep polygraph to measure the amount of time taken for falling asleep (sleep latency). The implement of both MSLT and MWT requires the facility and equipment for sleep polygraph and a skilled tester. So that it is difficult to use them in-vehicle experiment.

Somnolence detection

Detecting somnolence methods can be either objective or subjective. The subjective methods include the Stanford sleepiness scale (SSS), the Karolinska Sleepiness Scale (KSS), and the visual analog scale (VAS). The methods are highly sensitive to the variations of sleepiness within an individual.

The objective methods also use physiological indices and driving-based information to assess the sleepiness state. Some physiological indices were used in the literature are: EEG, HRV, and the percentage closure of eyes averaged across a time (PERCLOS). The driving information which are considered correlated with the sleepiness are the lane deviation and lateral acceleration.

6.4 Preliminary results

The HR data was extracted from the raw ECG data. Then the mean values of HR in 5-second segments were calculated. The data was then aligned with the marker data collected from the video file. Figure 6.3 and 6.4 showed the results of the mean HR and drowsiness level of two participants in case of awake and sleepiness. The preliminary results showed that the mean HR decrease at the start of the somnolence and increase at the end of the period (Figure 6.5). This finding consistent with the report that the HR decrease in the case of fatigue and low arousal level, which is also the drowsiness state.

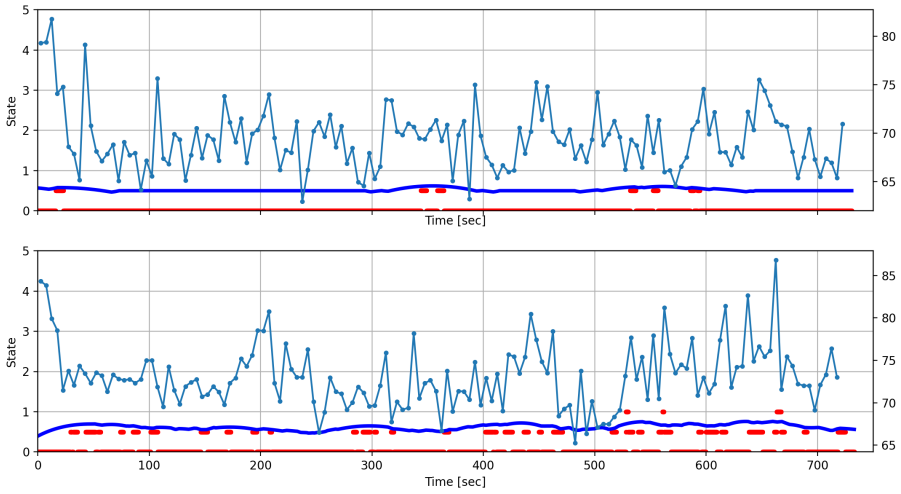

Figure 6.3: Subjects' heart rate in awake driving

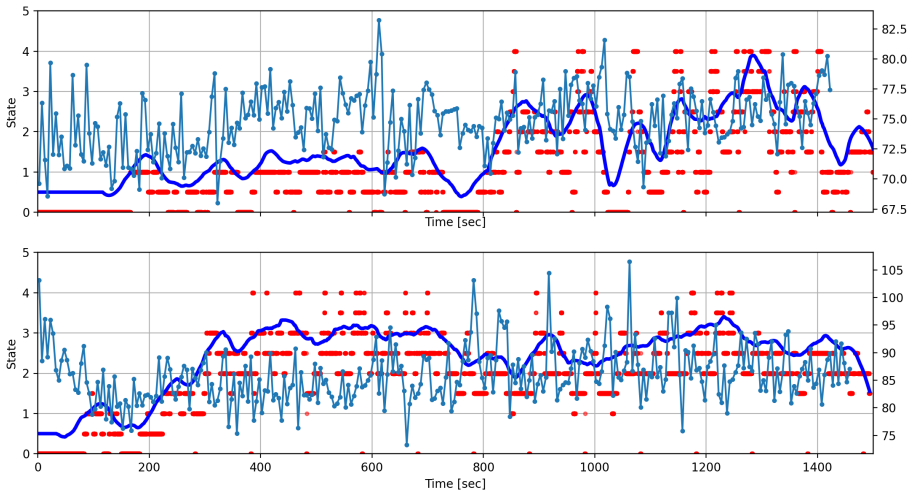

Figure 6.4: Subjects' heart rate in sleepiness driving

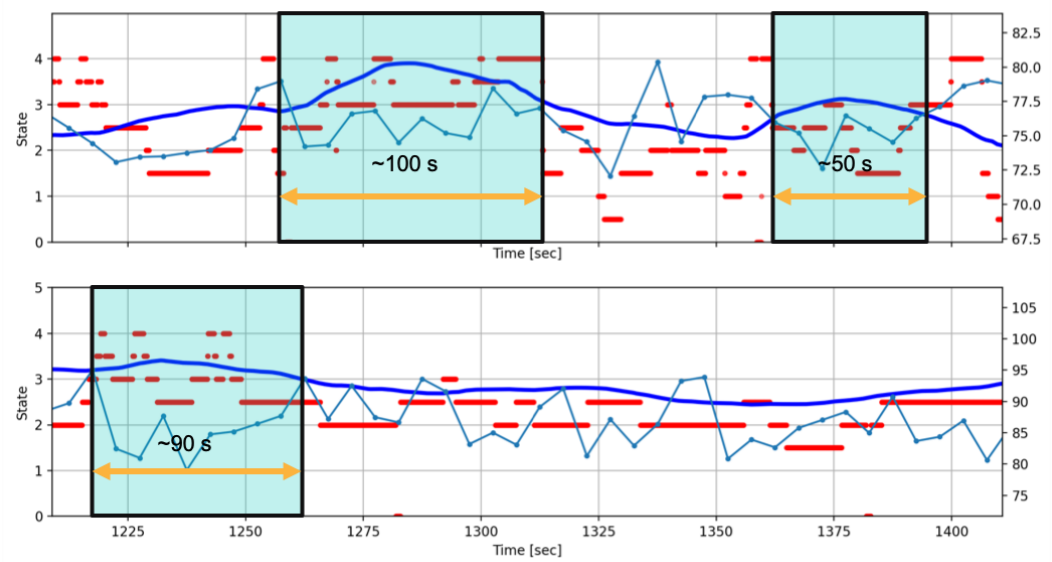

Figure 6.5: Heart rate decrease in high drowsiness level

6.5 Conclusion

In this chapter, the study about drowsiness has been conducted. This is an on-going study and not finished yet. The preliminary results showed that drowsiness could be detected by using the data acquired in the experiment. It can be seen that the graphical method used in Chapter 5 in case the driver states change significantly. But in the case of somnolence detection, the state changes from awake to drowsiness more gradually. So that more considerations need to be taken in using the physiological indices and driving information to detect drowsiness by using the graphical model.

Chapter 7

Driver assistance system

7.1 Background

Driving is always considered as a complex task which requires both physical and cognitive activities. Driving for a too long period or under cognitive stressors can increase the chance of accidents.The physical disorder or diseases are also considered as a factor which also increases the risk of accidents (Schultheis et al. , 2011). Researchers and automakers have cooperated to provide the vehicle with options to reduce both the physical and cognitive workload of the driver. But the number of intrinsic sudden death in traffic accidents is still high over the years (Table 7.1).

Table 7.1: Report of intrinsic sudden death of driver

Author	Location	Period	Sudden death reported	
			Number	Percentage
West et al. , 1968	USA(California)	1963-1965	155/1026	15%
Osawa et al. , 1998	Japan(Kanagawa)	1992-1997	15/188	8%
Oliva et al. , 2011	Canada	2002-2006	123/1260	9.7%
Tervo et al. , 2013	Finland	2008-2009	55/488	11.3%

Among the natural cause of sudden death, cardiovascular disease (CVD) and cerebrovascular disease are statistically found the most common causes while driving(Schmidt et al. , 1990; Motozawa et al. , 2005). The effects of cardiovascular diseases are not immediate but gradual, so that the driver can somehow stop the vehicle to the side of the road safely. The common symptoms of heart disease are chest pain or discomfort (angina), shortness of breath, pain or numbness in legs or arms or shoulder, dizziness or fatigue, or abnormal drowsiness. Those symptoms can impair the awareness, recognition, eyesight, physical strength, and other functions that will result the distracted driving. Another more serious symptom that comes with CVD is syncope, the sudden and transient loss of consciousness, will lead to the lost control of the vehicle. The relationship between driving accidents and heart disease has been studied for many years (West et al. , 1968; Baker and Spitz , 1970; Tervo et al. , 2013). In Europe, a meta-analysis has reported that CVD patients have 23% higher chance of involving accident than drivers without the disease (Gma et al. , 2003). In Japan, Motozawa et al. , 2005 have reported that the main cause of natural death after the wheel is ischemic heart disease based on the autopsies results of the Transportation Bureau of National Police Agency (Japan). Even though, the Japanese cardiovascular disease mortality is relatively low, but there is an increasing trend of heart disease incidence in urban men (Iso , 2011).

To prevent the effect of health disease on driving capability, the authorities have issued laws and regulations to decide whether a person with heart disease is safe to drive or not (Epstein et al. , 1996; Petch , 1998; Theodoros A. Zografos , 2010). Drivers who want to renew driving license need to pass a screening questionnaire and test for both physical and cognitive functions. Although these methods can prevent several deaths at the wheel caused by CVD, there are still drivers who are healthy or seem healthy but have a potential to get cardiac events or emergencies when driving.

7.2 System Objectives

The objective of this study is to develop a concept system that can prevent traffic accidents caused by physical disorders specifically cardiac emergencies. The system can detect driver's abnormality by collecting the biosignals and driver's ergonomic features: ECG data, PPG data, blood pressure, by using a steering-type sensor, and the driver's posture by using a driver agent and camera. In case of the driver lost his or her capability to drive, the system will take over the maneuver of the vehicle, and automatically drive to a safe spot. Figure 7.1 shows the 3 phase of the system operation:

- **Phase 1:** Normal driving
- **Phase 2:** Cardiac emergency detection
- **Phase 3:** Automated stop & E-call

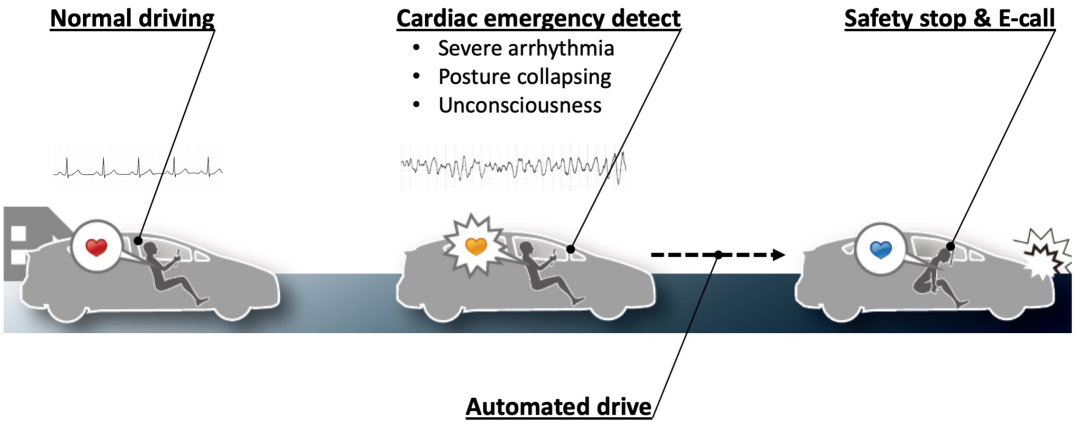

Figure 7.1: System objectives

7.3 System configuration

7.3.1 Bio-signal sensing and emergency event detection

To detect the CVD event, the biosignals play an essential part. In the medical field, the data is often collected from the electrodes attached to the subject's chest. In this concept system, the ECG electrodes and PPG sensor are attached on the outer frame of the steering wheel. By gripping the steering wheel with both hands and place the right thumb on the PPG sensor, ECG data is recorded and blood pressure (BP) is estimated from the pulse transmit time by both ECG and PPG data. Figure 7.2 shows the position of the sensors on the wheel.

The abnormality in the rhythm of ECG data is called arrhythmia. During the arrhythmia, the heart can beat faster (tachycardia) or slower (bradycardia) or has an irregular rhythm (abnormality of QRS or irregular of RR or blood pressure). These abnormal states of the heart will make the driver feel uncomfortable and lose concentration or capability to operate the vehicle properly. In serious cases, arrhythmia can lead to life-threatening complications such as stroke, heart failure, or sudden cardiac arrest. The system will detect the abnormal ECG, PPG and BP and trigger the emergency signal to the next unit.

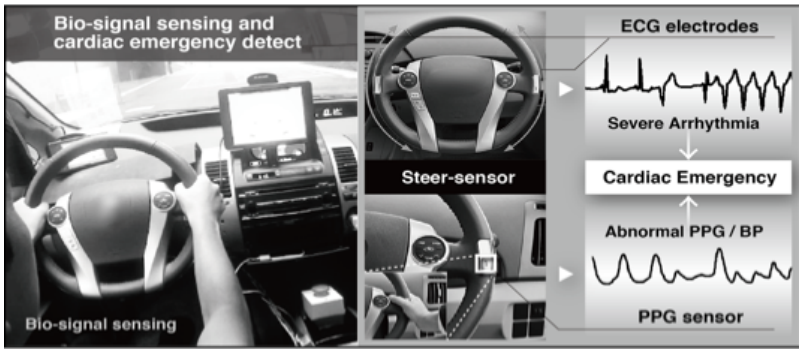

Figure 7.2: ECG & PPG signals collected by the steer-sensor

7.3.2 Driver's ergonomic factor

When the system receives the abnormal detect signal in the driver's state sent from the biosensing unit, the driver-monitor camera will detect the driver's posture (Figure 7.3). Some kind of arrhythmias can cause pain or numbness in the chest area or on the shoulder, others make the driver feel dizziness, fatigue, or even loss consciousness. These phenomenons make the driver uncomfortable and eventually lose the normal driving posture. The abnormal posture will be captured by the monitoring camera.

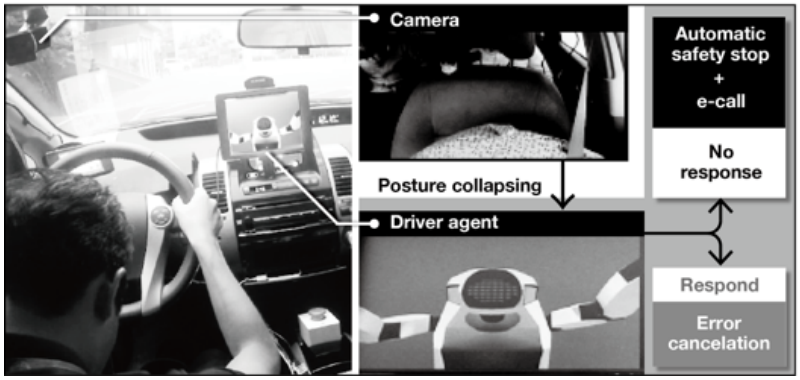

Figure 7.3: Posture collapsing detection

7.3.3 Driver agent assistance

A driver agent is equipped inside the vehicle in the shape of a robot putting on the dashboard in front of the driver. The driver agent has the functions of giving instructions and alerts while driving. If detect the abnormal posture, the driver agent will alert the driver. The alerting is designed to avoid the misdetection of the arrhythmia and posture collapsing. In case of false detection, the driver can override the system by confirming that he or she is alright. In case of true detection, after a certain period, the driver cannot react to the agent, the autonomous drive mode is activated , and then call to the emergency center.

7.3.4 Automated driving system

Many subsystems in the automated driving system enable the vehicle to "sense" the surrounding environment: a LiDAR sensor (HDL-64E, Velodyne LiDAR, Inc.), 360 degrees camera (Ladybug 5, Point Grey Research, Inc.), Grasshoper 3 cameras and Javad RTK sensors receive GPS (Global Positioning System) information from satellites as shown in the Figure 7.4. The sensors fusion in the system allows the precision of the estimated position within 0.1 meters. This configuration enables the vehicle to operate in both urban and suburban areas. The system can also automatically stop in front of or avoid humans and other obstacles on the road by itself. When the life-threatening state is confirmed by both prior units: the biosensing and the driver agent (including the posture camera), the system will activate the automated driving mode. In autonomous driving, the system recognizes the surrounding environment of the vehicle by the sensors and the premade map. In this case, the system also can find a safety spot to on the side of the road to park the vehicle. Figure 7.5 shows the decision-making procedure of the shifting from manual to automated mode.

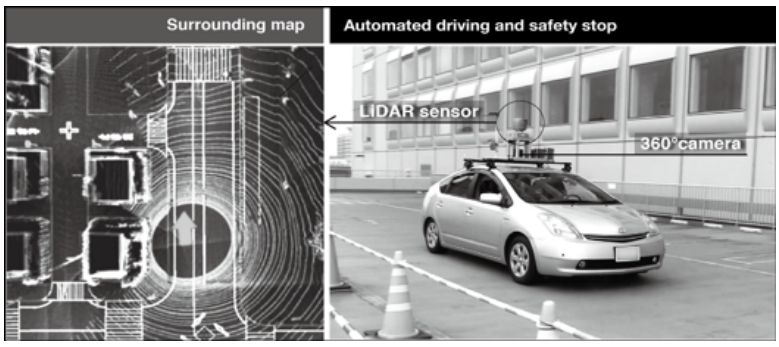

Figure 7.4: Automated driving system

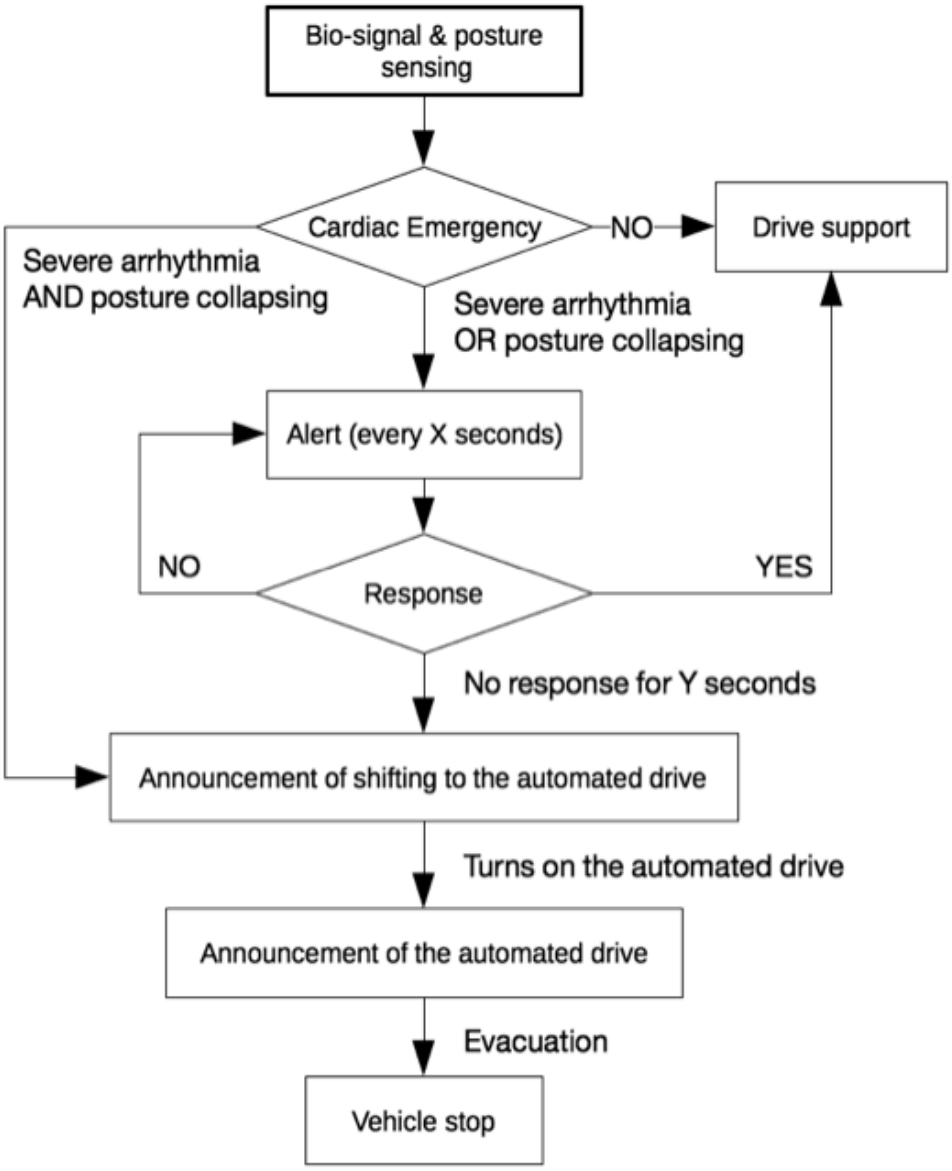

Figure 7.5: Decision-making procedure

7.4 Demonstration

The demonstration of the system concept has been presented at TOC Ariake, Tokyo, Japan in August 2015. A well-prepared scenario was set to demo the working prototype: Two test drivers seat inside the vehicle, one demo driver will seat on the passenger seat to perform the simulated abnormal state, the other assistance driver will seat on the driver seat to take countermeasures in case of system errors. The steer-sensor and the driver-monitoring camera were attached on the passenger seat side as shown on the Figure 7.6.

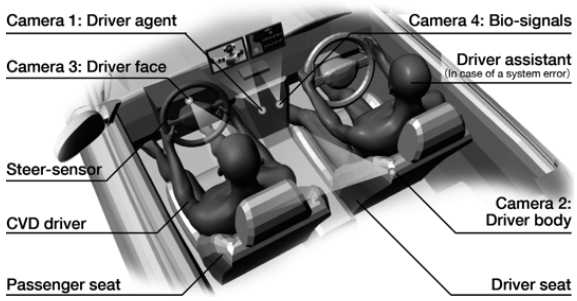

Figure 7.6: Interior layout of the vehicle

The demo driver drove in a healthy state and the abnormal state was injected into the system to emulate the emergency. Normal ECG data was measured directly by the sensor on the steering wheel. The emergency ECG (Ventricular fibrillation - VF) was obtained from PhysioBank MIMIC database (Moody and Mark , 1996) and used for simulation of the life-threatening situation.

The threshold crossing sample count (TCSC) (Arafat et al. , 2011) was implemented to detect the VF signal. Monitoring cameras were settled inside the vehicle for checking and showing of what happens during the demonstration: two cameras for driver's face and posture detection, one for the driver agent animation and one for the demo driver's biosignals (Figure 7.7). The scenario of the demonstration is illustrated in Figure 7.8. The demonstration started with normal driving and

the system worked in the normal state. The arrhythmia detection and cameras worked from the beginning and continuously monitored the biosignals for abnormal symptoms. Right after the simulated VF was injected, the arrhythmia was detected by the emergency detection unit and the posture collapsing of the driver was detected by the face camera and driver agent. The agent gave an alert to the driver to confirm the situation. Then the system automatically turned on the automated driving when it confirms the driver's critical state. In the driving scene, the automated driving system successfully recognized a pedestrian crossing the road and stopped in front of him, waiting until he finished crossing. As soon as the system confirmed that there were no obstacles ahead; the automated driving system drove the vehicle to the safe parking area (Evacuation space on side of the road) and stopped the vehicle.

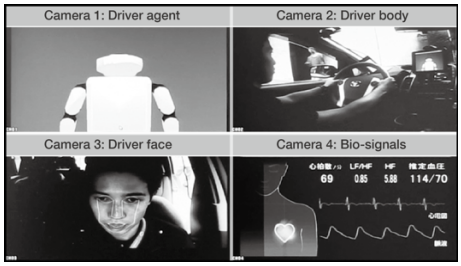

Figure 7.7: Captured cameras at the demonstration

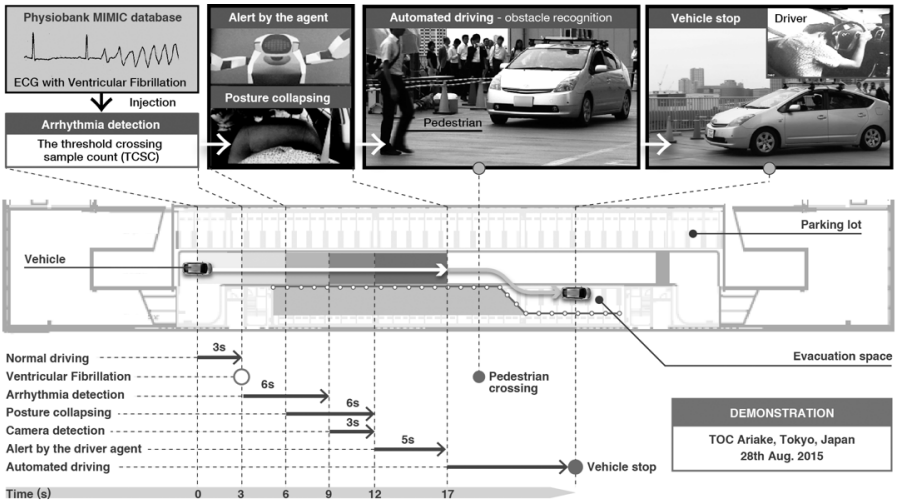

Figure 7.8: The scenario of the demonstration

7.5 Results

The demonstration vehicle started at the speed of 20 km/h, it took some seconds for the vehicle to reach the designated velocity and all the system started with the normal state. The system successfully detected the simulated abnormal state and automatically maneuvered the vehicle right after confirming the unfitness of the driver to the safety spot on the side of the road.

The European automakers have developed similar systems in recent years (Volkswagen , 2016). The system prevents the frontal crash and lane departures by using adaptive cruise control and a lane-keep assist when a driver lost his capacity to drive by a physical disorder. Another related system demonstration has been presented at the 22nd ITS world congress, France, in October 2015 (AISIN SEIKI Co.Ltd. , 2015). The system used a camera to detect the driver's incapacity and automatically stopped the vehicle on the shoulder of a road at the demonstration. Automakers also introduced systems which enable the elder driver stay safe with the similar functions (BMW). Although the related systems are well designed for the countermeasures for incapacitated drivers, the future studies require further detection methodologies of the driver's abnormality at earlier stage. A few seconds of early detection can be critical to deciding the dead or alive of the driver. The prototype of the system using bio-signal detection was successfully demonstrated its function at the prepared scenario.

Limitation

In the demonstration, the concept system also revealed its limitations and problems.

- **Sensor noise**: Conventional ECG sensor in a separated test has showed that the driving condition actively adds noise to the signal. Motion artifacts due to bodily movement were detected as severe arrhythmias, resulting in misdetec-

tions. The steer-sensor sometimes generates more noises than the conventional sensors and the waveform of the PQRST complex easily gets distorted.

- **Getting data**: In practical driving, it is hard to find the driver gripping the driving wheel by both hands all the time. Sometimes the driver will do the other task and just drive with one hand, or just simple feeling comfortable with driving one hand. In such cases, it requires alternative or additional sensors such as capacitive ECG sensor or wearable PPG sensor to compensate for the signal distortions or the signal losses.

- **Decision making**: It can be seen from Figure 7.8, the period of the uncontrolled is around 14 seconds with the initial velocity when the arrhythmia started was 20 km/h (5.6 m/s). As a result the freely moving distance is roughly 78 meters. Normally, if the driver feels any discomfort while driving he or she will apply brake and slow down. Others might suffer more serious symptoms and collapse. The unconscious driver can accidentally push his or her foot on the acceleration pedal and suddenly make the vehicle travel faster or leaning to the steering wheel the vehicle to one side and lead the vehicle hitting to the side of the road. Those situations will eventually lead to serious accidents. It is important to shorten the detection time of both arrhythmia and posture collapse. In that case, algorithms or methods which can predict arrhythmia or even prevent before it happens play an essential part in the system.

7.6 Overcome the limitations

The concept of the system at the time demonstrated still had limitations. The limitation of the sensor was due to the limitation of the current technologies. With the current development of sensor, portable ECG devices are available, that means there is no need the steering-type sensor. Normal daily use is acceptable but more attention when using in vehicle due to the potential noise comes from the body movement while driving and the seatbelt. Another potential candidate is using PPG sensor. PPG sensors are embedded in many wearable devices such as wrist-watch, glasses, and earphone. Even though PPG sensors have not reached the medical standard but their data keeps an important part in detect driver state and driver health status.

As for the decision making, it can be seen that detect the emergency situations is not enough. Using framework such as risk estimation or case study estimating technique, detecting sudden events and gradual events while driving could improve the safety of the driver assistance system by continuously monitoring the driver health status. Figure 7.9 briefly illustrates the concept.

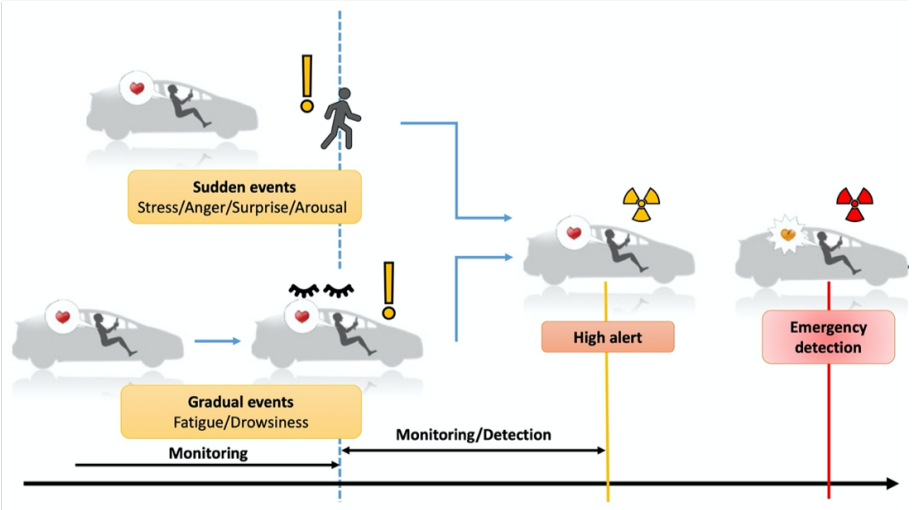

Figure 7.9: Strategy to improve the health monitoring system

7.7 Conclusion

This chapter has demonstrated the concept of an automated safety stop system in case of cardiac emergencies. At the time of proposal (2016), the prototype system has shown possibilities benefits to not only patients but also normal healthy people. Even though the system contains some limitations (sensors, decision making), possible solutions were proposed. By using the graphical-based models proposed in Chapter 5, detecting the sudden events (abrupt stressors) and gradual events (gradual symptoms or sign symptoms) during driving can improve the effectiveness of the driver assistance system.

Chapter 8

Conclusion

8.1 Conclusion

The main purpose of the study is to proposed a method to estimate the driver states by using non-invasive sensors and in-vehicle data. The results of the study show that this objective has been fulfilled.

Firstly, the driver state assessment methods have been investigated: physiological indices, driving-based methods, and subjective questionnaires. By choosing the proper indices for the specific experiment, the effects of driving tasks and non-driving tasks to the physiological indices has been investigated in real-world test track. The results showed that driving tasks and secondary task have significant effects on the cardiac system. The heart rate and some HRV indices are sensitive to the driving situation. They can be used as indicators to detect driver state while driving.

Secondly, graphical models are introduced in this study with their advantages in exploring the interaction between components of the system structure. By applying the graphical model to the detection of the surprise state in case of misapplications, the detection outcome showed favorable results. In addition, the exploratory characteristic allows inferring the relationship between reaction time and the alert types. This result will help to improve the human-machine interface system in the future. The graphical model approach showed the potential of using in case of grad-

ual changes such as drowsiness detection.

Lastly, a concept of an automated safety safety stop system has been considered and demonstrated. The demonstration result proved that the system concept is good and can be used in the near future. Even though the driver assistance system still has some limitations, the possible solutions were discussed and could be overcome by using the proposed graphical model to detect driver states in the early stage of driving.

The autonomous vehicle is considered as the future of the automotive. But to achieve that Level 5 of autonomous, it will take a long time with the transition to the highly advanced driver assistance system (Level 3 and 4). The graphical model and the concept of driver health monitoring will contribute largely to keeping the driving safe. Even reaching that Level 5, monitoring vehicle passenger health still play an important role in the transportation industries.

8.2 Remarks for Future work

The main limitations of this study were the small sample size in generating the model. This limitation can increase the uncertainty of the estimated model. Therefore, caution should be taken in when applying this method to the other situations. The proposed model has been worked well in case the state change is abrupt. In case of gradual change such as drowsiness detection, more attention needs to be considered.

In the future, to confirm the robustness of the model, it is need to recruit a larger sample data and apply multiple model selection/average techniques to acquire the best model.

Bibliography

U. R. Acharya, J. S. Suri, J. A. Spaan, and S. Krishnan. *Advances in Cardiac Signal Processing*. 2007.

AISIN SEIKI Co.Ltd. Aisin Group to exhibit at 22nd ITS World Congress Bordeaux 2015, 2015.

H. Akihiro. ITARDA INFORMATION No. 124 - Accidents due to the misapplication of accelerator and brake pedals. Technical report, 2018.

H. Aoki and N. V. Q. Hung. Perceptual Risk Estimate for Collision Avoidance by Braking and Steering. (1):1–5, 2011.

M. A. Arafat, A. W. Chowdhury, and M. K. Hasan. A simple time domain algorithm for the detection of ventricular fibrillation in electrocardiogram. *Signal, Image and Video Processing*, 5(1):1–10, 2011.

S. P. Baker and W. U. Spitz. An evaluation of the hazard created by natural death at the wheel. *New England Journal of Medicine*, 283(8):405–409, 1970.

E. Belilovsky, G. Varoquaux, and M. Blaschko. Testing for differences in Gaussian Graphical Models: Applications to brain connectivity. In *Advances in Neural Information Processing Systems*, pp. 595–603, 2016.

S. Benedetto, M. Pedrotti, L. Minin, T. Baccino, A. Re, and R. Montanari. Driver workload and eye blink duration. *Transportation Research Part F: Traffic Psychology and Behaviour*, 14(3):199–208, may 2011.

N. Bhushan, F. Mohnert, D. Sloot, L. Jans, C. Albers, and L. Steg. Using a Gaussian graphical model to explore relationships between items and variables in environmental psychology research. *Frontiers in Psychology*, 10(MAY):1050, may 2019. URL https://www.frontiersin.org/article/10.3389/fpsyg.2019.01050/full.

BMW. SmartSenior : Intelligent services for senior citizens. p. 80788.

E. R. Boer. Behavioral Entropy As a Measure of Driving Performance. *International Driving Symposium on Human Factors in Driver Assessment, Training and Vehicle Design*, 1:p. 225–229, 2001. URL http://drivingassessment.uiowa.edu/DA2001/44{_}boer{_}edwin.pdf.

J. E. Bronson, J. M. Hofman, J. Fei, R. L. Gonzalez, and C. H. Wiggins. Graphical models for inferring single molecule dynamics. *BMC Bioinformatics*, 11(SUPPL. 8):1–10, oct 2010. URL https://link.springer.com/articles/10.1186/1471-2105-11-S8-S2https://link.springer.com/article/10.1186/1471-2105-11-S8-S2.

J. L. Campbell, C. M. Richard, J. L. Brown, and M. McCallum. Crash warning system interfaces: Human Factors insight and lessons learned. Technical Report January, 2007.

N. V. Chawla, K. W. Bowyer, L. O. Hall, and W. P. Kegelmeyer. SMOTE: Synthetic Minority Over-sampling Technique. *Journal of Artificial Intelligence Research*, 16:321–357, jun 2011. URL http://arxiv.org/abs/1106.1813http://dx.doi.org/10.1613/jair.953.

T. Danisman, I. M. Bilasco, C. Djeraba, and N. Ihaddadene. Drowsy driver detection system using eye blink patterns. In *2010 International Conference on Machine and*

Web Intelligence, ICMWI 2010 - Proceedings, pp. 230–233, 2010. URL https://hal.archives-ouvertes.fr/hal-00812315.

R. J. de Boer and K. Hurts. Automation Surprise: Results of a Field Survey of Dutch Pilots. *Aviation Psychology and Applied Human Factors*, 7(1):28–41, 2017. URL https://www.researchgate.net/publication/317112664.

T. D'Orazio, M. Leo, C. Guaragnella, and A. Distante. A visual approach for driver inattention detection. *Pattern Recognition*, 40(8):2341–2355, aug 2007.

S. Epskamp, L. J. Waldorp, R. Mõttus, and D. Borsboom. The Gaussian Graphical Model in Cross-Sectional and Time-Series Data. *Multivariate Behavioral Research*, 53(4):453–480, 2018. URL http://www.tandfonline.com/action/journalInformation?journalCode=hmbr20.

A. E. Epstein, W. M. Miles, D. G. Benditt, a. J. Camm, E. J. Darling, P. L. Friedman, A. Garson, J. Collins, G. a. Kidwell, G. J. Klein, P. a. Levine, E. Francis, E. N. Prystowsky, and B. L. Wilkoff. Personal and Public Safety Issues Related to Arrhythmias That May Affect Consciousness : Implications for Regulation and Physician Recommendations. *Circulation*, 94:1147–1166, 1996.

M. R. Esco and A. a. Flatt. Ultra-short-term heart rate variability indexes at rest and post-exercise in athletes: Evaluating the agreement with accepted recommendations. *Journal of Sports Science and Medicine*, 13(3):535–541, 2014.

M. Fakhrhosseini, M. Jeon, and R. Bose. Estimation of drivers' emotional states based on neuroergonmic equipment: An exploratory study using fNIRS. In *Adjunct Proceedings of the 7th International Conference on Automotive User Interfaces and Interactive VehicularApplications, AutomotiveUI 2015*, pp. 38–43, 2015.

A. Farasat, A. Nikolaev, S. N. Srihari, and R. H. Blair. Probabilistic graphical mod-

els in modern social network analysis. *Social Network Analysis and Mining*, 5(1): 1–18, 2015. URL https://www.researchgate.net/publication/283450358.

G. M. Fitch, M. Blanco, J. F. Morgan, and A. E. Wharton. Driver Braking Performance to Surprise and Expected Events. *Proceedings of the Human Factors and Ergonomics Society Annual Meeting*, 54(24):2075–2080, 2012. URL https://www.researchgate.net/publication/266491470.

L. Fletcher and A. Zelinsky. Driver Inattention Detection based on Eye Gaze—Road Event Correlation. *The International Journal of Robotics Research*, 28(6):774–801, jun 2009. URL http://journals.sagepub.com/doi/10.1177/0278364908099459.

G. J. Forkenbrock and A. S. Snyder. NHTSA's 2014 Automatic Emergency Braking Test Track Evaluations. Technical Report June, 2015. URL https://www.researchgate.net/publication/267701201http://www.faa.gov/library/online{_}libraries/aerospace{_}medicine/sd/media/Wickens2.pdf.

Y. Forster, F. Naujoks, A. Neukum, and L. Huestegge. Driver compliance to takeover requests with different auditory outputs in conditional automation. *Accident Analysis and Prevention*, 109:18–28, dec 2017.

C. Gantiva, A. Araujo, L. Calderón, P. Gómez, and F. Reina. Psychophysiological responses to facial expression of surprise, sadness, and disgust. *Australian Journal of Psychology*, 71(2):100–107, 2019.

C. N. O. Gma, T. Vaa, T. Economics, J. Alvarez, and B. Hockey. *Impairments, Diseases, Age and their Relative Risks of Accident Involvement: results from meta-analysis, IMMORTAL*. Number August. 2003.

M. Gonçalves, R. Amici, R. Lucas, T. Åkerstedt, F. Cirignotta, J. Horne, D. Léger, W. T. McNicholas, M. Partinen, J. Téran-Santos, P. Peigneux, and L. Grote. Sleepiness at the wheel across Europe: a survey of 19 countries. *Journal of Sleep Research*, 24(3):242–253, jun 2015. URL http://doi.wiley.com/10.1111/jsr.12267.

M. Green. How Long Does It Take to Stop? Methodological Analysis of Driver Perception-Brake Times. *Transportation Human Factors*, 2(3):195–216, sep 2000. URL http://www.tandfonline.com/doi/abs/10.1207/STHF0203{_}1.

S. G. Hart. NASA-task load index (NASA-TLX); 20 years later. In *Proc. of the Human Factors and Ergonomics Society*, pp. 904–908, 2006.

M. Hours, E. Fort, P. Charnay, M. Bernard, J. L. Martin, D. Boisson, P. O. Sancho, and B. Laumon. Diseases, consumption of medicines and responsibility for a road crash: A case-control study. *Accident Analysis and Prevention*, 40(5):1789–1796, sep 2008.

H. Iso. Lifestyle and Cardiovascular Disease in Japan. *Journal of Atherosclerosis and Thrombosis*, 18(2):83–88, 2011. URL http://joi.jlc.jst.go.jp/JST.JSTAGE/jat/6866?from=CrossRef.

P. Kathirvel, M. Sabarimalai Manikandan, S. R. M. Prasanna, K. P. Soman, M. S. Manikandan, S. R. M. Prasanna, K. P. Soman, M. Sabarimalai Manikandan, S. R. M. Prasanna, and K. P. Soman. An Efficient R-peak Detection Based on New Nonlinear Transformation and First-Order Gaussian Differentiator. *Cardiovascular Engineering and Technology*, 2(4):408–425, 2011. URL https://link.springer.com/content/pdf/10.1007{%}2Fs13239-011-0065-3.pdf.

R. J. Kiefer, C. A. Flannagan, and C. J. Jerome. Time-to-Collision Judgments Under Realistic Driving Conditions. *Human Factors: The Journal of the Human*

Factors and Ergonomics Society, 48(2):334–345, jun 2006. URL http://hfs.sagepub.com/cgi/doi/10.1518/001872006777724499.

S. Klauer, T. A. Dingus, V. L. Neale, J. Sudweeks, and D. Ramsey. The impact of Driver Inattention on Near-Crash/Crask Risk: An analysis using the 100-car naturalistic driving study data. Technical report, sep 2006. URL https://vtechworks.lib.vt.edu/bitstream/handle/10919/55090/DriverInattention.pdf?sequence=1http://www.ncbi.nlm.nih.gov/pubmed/5538471.

Y. Komada, T. Shiomi, K. Mishima, and Y. Inoue. Associated factors for drowsy driving among licensed drivers. *[Nippon kōshū eisei zasshi] Japanese journal of public health*, 57(12):1066–1074, dec 2010.

G. K. Kountouriotis, P. Spyridakos, O. M. Carsten, and N. Merat. Identifying cognitive distraction using steering wheel reversal rates. *Accident Analysis and Prevention*, 96:39–45, nov 2016.

K. Kozak, J. Pohl, W. Birk, J. Greenberg, B. Artz, M. Blommer, L. Cathey, and R. Curry. Evaluation of lane departure warnings for drowsy drivers. In *Proc. of the Human Factors and Ergonomics Society*, pp. 2400–2404, 2006.

S. K. Lal, A. Craig, P. Boord, L. Kirkup, and H. Nguyen. Development of an algorithm for an EEG-based driver fatigue countermeasure. *Journal of Safety Research*, 34(3):321–328, aug 2003.

A. Landman, E. L. Groen, M. M. van Paassen, A. W. Bronkhorst, and M. Mulder. Dealing With Unexpected Events on the Flight Deck: A Conceptual Model of Startle and Surprise. *Human Factors*, 59(8):1161–1172, 2017. URL https://journals.sagepub.com/doi/pdf/10.1177/0018720817723428.

J. Laska and M. Narayan. skggm 0.2.7: A scikit-learn compatible package for Gaussian and related Graphical Models. jul 2017. URL https://zenodo.org/record/830033{#}.XJUSBpgzbDc.

A. S. Le, M. Inagami, H. Hamada, T. Suzuki, and H. Aoki. Towards online detection of driver distraction: Eye-movement simulation based on a combination of vestibulo–ocular reflex and optokinetic reflex models. *Transportation Research Part F: Traffic Psychology and Behaviour*, 65:716–729, aug 2019.

Y. Liao, S. E. Li, W. Wang, Y. Wang, G. Li, and B. Cheng. Detection of Driver Cognitive Distraction: A Comparison Study of Stop-Controlled Intersection and Speed-Limited Highway. *IEEE Transactions on Intelligent Transportation Systems*, 17(6):1628–1637, jun 2016. URL https://www.researchgate.net/publication/290509869http://ieeexplore.ieee.org/document/7378954/.

S. Liu, J. Wang, and T. Fu. Effects of lane width, lane position and edge shoulder width on driving behavior in underground urban expressways: A driving simulator study. *International Journal of Environmental Research and Public Health*, 13 (10), 2016. URL www.mdpi.com/journal/ijerph.

K. H. Lococo, L. Staplin, C. A. Martell, K. J. Sifrit, L. TransAnalytics, and U. o. N. C. S. H. S. R. Center. Pedal Application Errors. Technical report, mar 2012. URL www.ntis.gov.

A. Luximon and R. S. Goonetilleke. Simplified subjective workload assessment technique. *Ergonomics*, 44(3):229–243, 2001. URL http://www.tandf.co.uk/.

G. Markkula and J. Engstrom. A steering wheel reversal rate metric for assessing effects of visual and cognitive secondary task load. *13th World Congress on Intelligent Transport Systems and Services*, 2006.

H. Masahide. ITARDA INFORMATION No. 107 - Preventing driving operation errors. Technical report, 2014.

A. D. McDonald, T. K. Ferris, and T. A. Wiener. Classification of Driver Distraction: A Comprehensive Analysis of Feature Generation, Machine Learning, and Input Measures. *Human Factors*, 62(6):1019–1035, sep 2020. URL `http://journals.sagepub.com/doi/10.1177/0018720819856454`.

J. Min, P. Wang, and J. Hu. Driver fatigue detection through multiple entropy fusion analysis in an EEG-based system. *PLOS ONE*, 12(12):e0188756, dec 2017. URL `https://dx.plos.org/10.1371/journal.pone.0188756`.

R. Mohebbi and R. Gray. Driver Reaction Time to Tactile and Auditory Rear-End Collision Warnings While Talking on a Cell Phone. 2009.

G. B. Moody and R. G. Mark. A database to support development and evaluation of intelligent intensive care monitoring. *Computers in Cardiology*, 23:657–660, 1996.

Y. Motozawa, T. Yokoyama, H. Masahito, and T. Shogo. Analysis of Sudden Natural Deaths While Driving with Forensic Autopsy Findings. *. . . Conference on the . . .*, pp. 1–6, 2005. URL `http://www-nrd.nhtsa.dot.gov/pdf/nrd-01/esv/esv19/Other/Print22.pdf`.

O. Nakayama, T. Futami, T. Nakamura, and E. R. Boer. Development of a steering entropy method for evaluating driver workload. *Proceedings of JSAE Annual Congress*, (724):5–8, 1999.

T. Nguyen, S. Ahn, H. Jang, S. C. Jun, and J. G. Kim. Utilization of a combined EEG/NIRS system to predict driver drowsiness. *Scientific Reports*, 7(1):1–10, mar 2017. URL `www.nature.com/scientificreports`.

M. S. Nomikos, E. Opton, and J. R. Averill. Surprise Versus Suspense in the Production of Stress Reaction. *Journal of Personality and Social Psychology*, 8(2 PART 1):204–208, 1968.

G. Obinata, S. Tokuda, and N. Shibata. Mental Workloads Can Be Objectively Quantified in Real-time Using VOR (Vestibulo-Ocular Reflex). 2008.

A. Oliva, J. Flores, S. Merigioli, L. LeDuc, B. Benito, S. Partemi, D. Arzamendi, O. Campuzano, T. L. Leung, A. Iglesias, M. Talajic, V. L. Pascali, and R. Brugada. Autopsy investigation and Bayesian approach to coronary artery disease in victims of motor-vehicle accidents. *Atherosclerosis*, 218(1):28–32, 2011.

S. Olsson and F. Noé. Dynamic graphical models of molecular kinetics. *Proceedings of the National Academy of Sciences of the United States of America*, 116(30): 15001–15006, 2019.

M. Osawa, T. Nagasawa, N. Yukawa, Y. Nakajima, Y. Seto, T. Ohki, T. Saito, and S. Takeichi. Sudden natural death in driving: Case studies in the western area of Kanagawa. *Japanese Journal of Legal Medicine*, 52(5):315–318, oct 1998. URL `http://www.ncbi.nlm.nih.gov/pubmed/10077978`.

D. Paz-Linares, E. Gonzalez-Moreira, J. Bosch-Bayard, A. Areces-Gonzalez, M. L. Bringas-Vega, and P. A. Valdés-Sosa. Neural connectivity with hidden gaussian graphical state-model, 2018.

L. Pecchia, R. Castaldo, L. Montesinos, and P. Melillo. Are ultra-short heart rate variability features good surrogates of short-term ones? State-of-the-art review and recommendations. *Healthcare Technology Letters*, 5(3):94–100, 2018. URL `http://creativecommons.`

F. Pedregosa, R. Weiss, M. Brucher, G. Varoquaux, A. Gramfort, V. Michel, B. Thirion, O. Grisel, M. Blondel, P. Prettenhofer, R. Weiss, V. Dubourg, J. Van-

derplas, A. Passos, D. Cournapeau, M. Brucher, M. Perrot, and É. Duchesnay. Scikit-learn: Machine Learning in Python. *Journal of Machine Learning Research*, 12:2825–2830, 2011. URL http://scikit-learn.sourceforge.net.http://jmlr.csail.mit.edu/papers/v12/pedregosa11a.html{%}5Cnhttp://arxiv.org/abs/1201.0490.

Y. Peng, L. N. Boyle, and S. L. Hallmark. Driver's lane keeping ability with eyes off road: Insights from a naturalistic study. *Accident Analysis and Prevention*, 50:628–634, 2013. URL https://reader.elsevier.com/reader/sd/pii/S0001457512002370?token=3142BD19567DFB0DC0A7A70AC3CFF3891BA0D7778B7D576E91BD7BD2E3F3B2AD634EE87A520CD6BD7

M. C. Petch. Driving and heart disease, Prepared on behalf of the Task Force by M. C. Petch. *European Heart Journal*, 19(8):1165–1177, aug 1998.

G. B. Reid and T. E. Nygren. The Subjective Workload Assessment Technique: A Scaling Procedure for Measuring Mental Workload. *Advances in Psychology*, 52 (C):185–218, jan 1988.

J. Rivera, A. B. Talone, C. T. Boesser, F. Jentsch, and M. Yeh. Startle and Surprise on the Flight Deck. *Proceedings of the Human Factors and Ergonomics Society Annual Meeting*, 58(1):1047–1051, sep 2014. URL http://journals.sagepub.com/doi/10.1177/1541931214581219.

E. Roidl, B. Frehse, and R. Höger. Emotional states of drivers and the impact on speed, acceleration and traffic violations - A simulator study. *Accident Analysis and Prevention*, 70:282–292, sep 2014.

D. Schleuning and Y. Douglas. Preferred time-headway of highway drivers. 2001. URL https://www.researchgate.net/publication/3913786.

P. Schmidt, K. Haarhoff, and W. Bonte. Sudden natural death at the wheel - A particular problem of the elderly? *Forensic Science International*, 48(2): 155–162, dec 1990. URL http://linkinghub.elsevier.com/retrieve/pii/037907389090108B.

R. A. Schmidt, D. E. Young, T. J. Ayres, and J. R. Wong. Pedal Misapplications: Their Frequency and Variety Revealed through Police Accident Reports. *Proceedings of the Human Factors and Ergonomics Society Annual Meeting*, 41 (2):1023–1027, oct 1997. URL https://search.proquest.com/docview/235467916/fulltext/4E313C7B5A8B4DDAPQ/1?accountid=12653http://triodyne.com/fosset/schmidt{_}1997.pdfhttp://journals.sagepub.com/doi/10.1177/107118139704100266.

M. T. Schultheis, J. DeLuca, and D. Chute. *Handbook for the assessment of driving capacity*. Academic Press, 2011.

F. W. Siebert, M. Oehl, and H. R. Pfister. The influence of time headway on subjective driver states in adaptive cruise control. *Transportation Research Part F: Traffic Psychology and Behaviour*, 25(PART A):65–73, jul 2014.

C. Sinoquet. *Probabilistic Graphical Models for Genetics, Genomics, and Postgenomics*. 2014. URL https://books.google.co.jp/books?hl=en{&}lr={&}id=Y-hjBAAAQBAJ{&}oi=fnd{&}pg=PP1{&}dq=graphical+models+chemistry{&}ots=CfBTuHzldZ{&}sig=zZTbFDMu0zNz1MGK4pcvtUxxrKg{#}v=onepage{&}q=graphicalmodelschemistry{&}f=false.

E. T. Solovey, M. Zec, E. A. Garcia Perez, B. Reimer, and B. Mehler. Classifying driver workload using physiological and driving performance data. *Proceedings of the 32nd annual ACM conference on Human factors in computing systems - CHI*

'14, pp. 4057–4066, 2014. URL http://www.scopus.com/inward/record.url?eid=2-s2.0-84900446066{&}partnerID=tZOtx3y1.

T. Tamura. Current progress of photoplethysmography and SPO2 for health monitoring, feb 2019. ISSN 2093985X. URL /pmc/articles/PMC6431353/?report=abstracthttps://www.ncbi.nlm.nih.gov/pmc/articles/PMC6431353/.

M. A. Tanveer, M. J. Khan, M. J. Qureshi, N. Naseer, and K. S. Hong. Enhanced drowsiness detection using deep learning: An fNIRS Study. *IEEE Access*, 7: 137920–137929, 2019. URL https://ieeexplore.ieee.org/stamp/stamp.jsp?arnumber=8846024.

G. Taoka. Brake reaction times of unalerted drivers. *ITE journal*, 59(3):19–21, 1989.

M. P. Tarvainen, J.-P. Niskanen, J. A. Lipponen, P. O. Ranta-aho, and P. A. Karjalainen. Kubios HRV – Heart rate variability analysis software. *Computer Methods and Programs in Biomedicine*, 113(1):210–220, 2014.

T. Tervo, E. Raty, P. Sulander, J. M. Holopainen, T. Jaakkola, K. Parkkari, E. Räty, P. Sulander, J. M. Holopainen, T. Jaakkola, and K. Parkkari. Sudden Death at the Wheel Due to a Disease Attack. *Traffic Injury Prevention*, 14(2):138–144, jan 2013. URL http://www.tandfonline.com/doi/abs/10.1080/15389588.2012.695827.

D. G. K. Theodoros A. Zografos. Review Article Guidelines and Regulations for Driving in Heart Disease. *Hellenic Journal of Cardiology*, 51:226–234, 2010.

S. Tsujita, A. Azuma, I. Tomoki, K. Aoki, A. Hirano, A. S. Le, T. T. Nguyen, H. Aoki, K. Shimazaki, T. Ikoma, K. Aoki, A. Hirano, S. L. Anh, T. T. Nguyen, K. Shimazaki, and H. Aoki. Effects of the HMI on Elderly Drivers' Behavior under a Simulated Unexpected Situation. In *2019 JSAE Annual Spring Congress*, 2019.

J. C. Verster and T. Roth. Excursions out-of-lane versus standard deviation of lateral position as outcome measure of the on-the-road driving test. *Human Psychopharmacology*, 29(4):322–329, jul 2014. URL http://doi.wiley.com/10.1002/hup.2406.

Volkswagen. Emergency Assist, 2016.

I. West, G. L. Nielsen, A. E. Gilmore, and J. R. Ryan. Natural Death at the Wheel. *JAMA: The Journal of the American Medical Association*, 205(5):266, jul 1968. URL http://jama.jamanetwork.com/article.aspx?doi=10.1001/jama.1968.03140310024005.

W.H.O. Global Status Report on Road Safety 2018: Summary. Technical report, 2018. URL http://apps.who.int/bookorders.http://apps.who.int/bookorders.{%}0Ahttps://www.who.int/violence{_}injury{_}prevention/road{_}safety{_}status/2018/GSRRS2018{_}Summary{_}EN.pdf.

W.H.O. Road traffic injuries. Technical report, World Health Organization, 2020. URL https://www.who.int/news-room/fact-sheets/detail/road-traffic-injuries.

C. D. Wickens. Multiple Resources and Mental Workload. *Human factors*, 50(3): 449–455, 2008.

L. Xu, B. Wang, G. Xu, W. Wang, Z. Liu, and Z. Li. Functional connectivity analysis using fNIRS in healthy subjects during prolonged simulated driving. *Neuroscience Letters*, 640:21–28, feb 2017.

K. Yoshino, M. Edamatsu, M. Yoshida, and K. Matsuoka. An algorithm for detecting startle state based on physiological signals. *Accident Analysis and Prevention*, 39 (2):308–312, mar 2007.

H. Zeng, C. Yang, G. Dai, F. Qin, J. Zhang, and W. Kong. EEG classification of driver mental states by deep learning. *Cognitive Neurodynamics*, 12(6):597–606, dec 2018. URL `https://doi.org/10.1007/s11571-018-9496-y`.

H. Zhang, K. Ke, W. Li, and X. Wang. Graphical models based hierarchical probabilistic community discovery in large-scale social networks. *International Journal of Data Mining, Modelling and Management*, 2(2):95–116, 2010.